Agricultural and Forest Meteorology 252 (2018) 192–207

Contents lists available at ScienceDirect

Agricultural and Forest Meteorology

journal homepage: www.elsevier.com/locate/agrformet

Canopy profile sensitivity on surface layer simulations evaluated by a multiple canopy layer higher order closure land surface model

Kuang-Yu Chang[a,b,c,*], Kyaw Tha Paw U[a], Shu-Hua Chen[a]

[a] Department of Land, Air and Water Resources, University of California, Davis, CA, USA
[b] Earth System Research Center, University of New Hampshire, Durham, NH, USA
[c] Climate and Ecosystem Sciences Division, Lawrence Berkeley National Laboratory, Berkeley, CA, USA

ARTICLE INFO

Keywords:
ACASA
Multiple canopy layer land surface model
AmeriFlux
Canopy profile sensitivity

ABSTRACT

The canopy structural and functional impacts on land surface modeling of energy and carbon fluxes were investigated by a series of simulations conducted at AmeriFlux eddy covariance sites. Canopy structures were described by different degrees of complexity of Leaf Area Index (LAI) datasets. The monthly climatological LAI datasets applied in the Weather Research and Forecasting (WRF) Model and the Community Earth System Model (CESM) were used to represent static ecological conditions. The LAI remotely sensed by the Moderate Resolution Imaging Spectroradiometer (MODIS) was used to represent time-varying ecological conditions with natural variability. To investigate the sensitivity of different canopy profile representations, all of these LAI datasets were used to assign the necessary ecological information for single and multiple canopy layer land surface models to simulate a seven-year period across a variety of vegetation covers. The results show that a more realistic canopy profile representation (i.e., multiple layers), both in terms of structural and functional treatments, improves biogeophysical and biogeochemical simulations. The root mean square errors for the simulated evapotranspiration and Net Ecosystem Exchange are reduced by 10% and 15%, respectively when the ecological information is represented by a more realistic time-varying LAI dataset instead of a static LAI dataset with no geographical sensitivity. A land surface model with multiple canopy layers and a realistic ecological dataset, which can better represent ecosystem structural and functional responses to microclimate conditions, is thus recommended for long-term climate projections.

1. Introduction

The terrestrial carbon sink accounts for more than one third of the annual global carbon sink in the atmosphere by plant photosynthetic carbon assimilation (Farquhar et al., 1993; Ciais et al., 1997; Sitch et al., 2003). Although the total terrestrial carbon sink is smaller than the oceanic carbon sink, the terrestrial carbon sink exhibits more variability in both space and time due to the more complex vegetation distribution and more prominent seasonality. This type of variability over land can be captured by implementing realistic vegetation type distribution and seasonal leaf area variation in land surface models (Bonan et al., 2002). Ecosystem response is dependent on ecophysiological processes that are strongly plant type and leaf area dependent (Gifford, 1974; Ball et al., 1987; Collatz et al., 1992, Mahowald et al., 2016). The plant species communities and the leaf area are usually represented by simplified representative ecosystems labeled as Plant Functional Types (PFT) each with a characteristic Leaf Area Index (LAI) (Bonan et al., 2002). Although PFTs are essential in determining ecosystem response mechanisms (Bunn and Goetz, 2006), they are usually assumed to be phenologically constant in surface vegetation datasets, that is the PFTs do not exhibit regular seasonal variations for the same geographical location. Seasonal variations in LAI is often prescribed in surface vegetation datasets, and LAI has been suggested to be one of the most important variables in global terrestrial carbon simulation due to its significant impacts on plant physiological and phenological processes (Murray-Tortarolo et al., 2013; Anav et al., 2013; Hardwick et al., 2015). Previous works on Amazon's deforestation highlighted the impacts from LAI changes on ecosystem responses through shifting the energy partition from available energy into sensible and latent heat fluxes and thus affecting atmospheric boundary layer development and local and regional circulation patterns (Foley et al., 2003; Knox et al., 2011; Fatichi et al., 2015). As a result, a more realistic high-resolution surface vegetation LAI dataset, such as those available from satellite observations (Carlson and Ripley, 1997; Yang et al., 2006), is expected to improve global terrestrial carbon simulation (Zhang et al., 2003 and Garrity et al., 2011).

* Corresponding author at: Climate and Ecosystem Sciences Division, Lawrence Berkeley National Laboratory, Berkeley, California, USA.
E-mail address: ckychang@lbl.gov (K.-Y. Chang).

https://doi.org/10.1016/j.agrformet.2018.01.027
Received 28 February 2017; Received in revised form 16 January 2018; Accepted 18 January 2018

Table 1
The AmeriFlux sites investigated in this study.

Site name	Vegetation type (IGBP)	Predominant species	Coordinates
Blodgett Forest (US-Blo)	Evergreen needleleaf Forest	Ponderosa pine	38.8952°N, 120.6327°W
Duke Forest Loblolly Pine (US-Dk3)	Evergreen needleleaf Forest	Loblolly pine	35.9782°N, 79.0942°W
Harvard Forest (US-Ha1)	Deciduous broadleaf	Red oak, red maple, black birch, white pine, and hemlock	42.5378°N, 72.1715°W
Howland Forest Main (US-Ho1)	Evergreen needleleaf Forest	Red spruce, and eastern hemlock	45.2041°N, 68.7402°W
Vaira Ranch (US-Var)	Grasslands	Purple false brome, smooth cat's ear, and rose clover	38.4067°N, 120.9507°W
Wind River Field Station (US-Wrc)	Evergreen needleleaf Forest	Douglas fir, and western hemlock	45.8205°N, 121.9519°W

Global surface vegetation datasets based on remotely sensed observations have been applied in models such as the Weather Research and Forecasting Model (WRF) and the Community Earth System Model (CESM) to improve surface layer simulation (Myneni et al., 2002; Myneni et al., 2003; Lawrence and Chase, 2007; Subin et al., 2011). However, the default settings in these models, to increase computational efficiency, only employ the monthly climatology global surface vegetation information to capture the general global vegetation distribution, and thus gloss over higher frequency LAI variations in space and time. This relatively static vegetation distribution approach comes with some uncertainties from inappropriate vegetation descriptions in long-term climate simulations (Levis et al., 2000; Diffenbaugh, 2005; Alo and Wang, 2010; Jeong et al., 2011; Yin et al., 2016). Recent studies, with single canopy layer models, have shown that more realistic LAI datasets are able to improve surface flux simulation and the predictions of drought conditions (Leuning et al., 2008; Ford and Quiring, 2013; Kumar et al., 2014; Hardwick et al., 2015). The realism of LAI datasets can have even stronger impacts in multiple canopy layer land surface models because the more sophisticated schemes could be more sensitive to real time canopy structure descriptions (Baldocchi and Wilson 2001; Ryder et al., 2016).

So far, few studies have discussed the sensitivity of multiple vertical canopy layer representations to turbulence fluxes simulation (Baldocchi and Wilson 2001; Kucharik et al., 2006; Ryder et al., 2016), and none of them employed higher order closure methods to accurately represent non-local turbulent transport that occurs in vegetated canopies.

In this study, we used a multiple canopy layer, higher order closure turbulent transfer model with detailed leaf physiology modules to investigate ecosystem response to natural canopy structural variations, driven by AmeriFlux site data. The site level scale was chosen to allow direct comparison between field measurements and model simulations. We proposed two hypotheses: (1) the temporal realism of canopy structural representation (mainly live LAI) is critical to land surface simulation; and (2) the realism of canopy functional parameterization is equally important. These hypotheses are linked to several different questions: How important are accurate turbulent parameterizations to overall fluxes? How important are multiple layers to fluxes? And, how important are the vertical profiles of scalars, with their potential to change ecophysiological response in each layer, to the overall fluxes? To examine hypothesis (1), we conducted a series of simulations with different descriptions of LAIs, e.g., more realistic time varying LAI versus static LAI datasets, at six AmeriFlux eddy covariance sites encompassing grassland, evergreen needleleaf forest and deciduous broadleaf forest across the continental United States. We examined hypothesis (2) by comparing the simulation results from land surface models with different levels of complexity in canopy process parameterization. These models ranged from a commonly used single layer land surface model with flux-gradient turbulent transfer physics, to a single layer canopy with higher order closure turbulence physics, to the end point in complexity of a multiple layer model with higher order closure turbulence physics. In all cases, the simulation results were then compared with AmeriFlux eddy covariance field measurements to test our hypotheses. The details of the models used in this study are given in Section 2, and descriptions of the six AmeriFlux sites and the chosen LAI datasets are given in Section 3. The simulation results and comparison to eddy covariance measurements are shown in Section 4, followed by discussion of results in Section 5, and ending in some concluding remarks.

2. Data

2.1. The AmeriFlux network, quality control and sites chosen

The AmeriFlux network was launched in 1996 to establish a dataset for carbon, water and energy fluxes in major climate and ecological biomes in North and South America based on eddy covariance measurements, with quality control and standardized data formats (Baldocchi et al., 2001). In this study, a range of microclimate and vegetation types were sampled by selecting six AmeriFlux sites across the continental United States, including four evergreen needleleaf forest sites, one broadleaf forest site and one C3 grassland site (Sections 2.1.1–2.1.6; Table 1), for the years 2000–2006. This time period was chosen to match the maximum available continuous data periods of the remotely sensed LAI by the Moderate Resolution Imaging Spectroradiometer (MODIS), and the meteorological and biological datasets at the six AmeriFlux sites.

Three quality control criteria were applied to the AmeriFlux network data. Data were omitted when (1) there was a rainfall event before or during the data collection period, which could have adversely affected sensor accuracy; (2) the observed frictional velocity was lower than 0.1 m/s (Reichstein et al., 2005), suggesting weak turbulence conditions in which two major problems could occur: (a) the eddy-covariance method might not accurately measure energy and carbon fluxes, and (b) fast response sonic anemometers could yield reduced accuracy, partially because of spatial resolution in their averaging volumes; and (3) the measured energy fluxes did not meet the energy balance closure criteria defined as the sum of sensible and latent energy within 20 percent error of the observed available energy, suggesting that there were potentially large errors associated with eddy covariance and/or net radiation and heat storage measurements. The philosophically supported use of the turbulent kinetic energy velocity scale or the standard deviation of the vertical wind velocity for indicating low turbulence regimes (Wharton et al., 2009) was not used because these measurements are not routinely available for the AmeriFlux sites. A brief description for the six AmeriFlux sites (Blodgett Forest, Duke Loblolly Pine Forest, Harvard Forest, Howland Forest, Wind River Forest, and Vaira Ranch Grassland) is given in the following paragraphs, and more detailed descriptions can be found on the AmeriFlux website (http://ameriflux.lbl.gov/).

2.1.1. Blodgett forest (USBlo)

The Blodgett Forest site (Goldstein et al., 2000) is located in El Dorado County, California, USA (38.8952°N, 120.6327°W). This site consisted of a mixed evergreen needleleaf forest dominated by ponderosa pine in a Mediterranean climate. The canopy height was 4 m when established in May 1997 with a growth rate of approximately 0.5 m/yr. The tower height was 10.5 m before February 2003 and changed to 12.5 m after that.

2.1.2. Duke forest loblolly pine (USDk3)

The Duke forest site (Lai and Katul, 2000) is located within the Blackwood Division near Durham, North Carolina, USA (35.9782°N, 79.0942°W). The uniform age overstorey at this site is almost solely composed of loblolly pines with an understory of 26 different hardwood species. The regional climate at this site is characterized by warm and humid summers and mild winters with an evenly distributed annual precipitation. The mean canopy height was 19 m measured at 2006, and the tower height was 22 m.

2.1.3. Harvard forest (USHa1)

The Harvard forest site (Moore et al., 1996) is located in Massachusetts, USA (42.5378°N, 72.1715°W). It is a deciduous broadleaf forest with dominant species including red oak, red maple, black birch, white pine and hemlock. The regional climate at the site is characterized by a cool and moist temperate climate with an annual precipitation around 110 cm distributed evenly throughout the year. The mean canopy height was 23 m, and the tower height was 30 m.

2.1.4. Howland forest (USHo1)

The Howland forest site (Hollinger et al., 1999) is located in central Maine, USA (45.2041°N, 68.7402°W). It is a needleleaf boreal-northern hardwood transitional forest with dominant species including red spruce (41%) and eastern hemlock (25%). The regional climate here is characterized by a cold, humid and continental climate with a snowpack existing of up to 2 m from December through the next March. The mean canopy height was 20 m and the tower height was 29 m.

2.1.5. Vaira ranch (USVar)

The Vaira Ranch site (Baldocchi et al., 2004) is located in the lower foothills of the Sierra Nevada Mountains in California, USA (38.4067°N, 120.9507°W). It is a grassland site dominated by C3 annual grasses. The regional climate is characterized by Mediterranean, and the majority of annual precipitation occurs from October to the next May corresponding to the growing season. The canopy height here varies with the maximum grass height that can reach up to 0.55 m during the peak growing season with a 0.12 m annual variation, and the instrument height was 2 m.

2.1.6. Wind River field station (USWrc)

The Wind River forest site (Paw U et al., 2004) is an evergreen needleleaf seasonal temperate rainforest located in south-central Washington state, USA (45.8205°N, 121.9519°W) representing the oldest North American AmeriFlux forest site at 400–500 years old. It contains fairly complex biomes, and the dominant overstorey species are Douglas Fir, and western hemlock, with lesser amounts of Pacific yew and Pacific silver fir. The regional climate is characterized by cold and moist winters and warm and dry summers. The mean canopy height was 56.3 m with the maximum height at 64.6 m, and the measurement height was 70 m.

2.2. The LAI datasets

In order to investigate canopy structural impacts on land surface simulations, we conducted our simulations with 3 different LAI datasets at the six AmeriFlux sites, to represent the effects of different descriptions of LAIs. The LAI datasets can be divided by their degrees of complexity into time-varying, climatology, and purely PFT dependent categories. The time-varying LAI dataset exhibits the details of intra-seasonal high frequency variations that are ignored in the coarse time resolution climatology and purely PFT dependent LAI datasets generally used in land surface models. All of these datasets were originally derived from the LAI products from the MODIS instrument mounted on the polar-orbiting Terra satellite. When compared with LAI field measurements, the root mean square error of the MODIS LAI products is around 0.66–1.53 m^2/m^2 (Yang et al., 2006; Fang et al., 2012).

The purely PFT dependent LAI dataset (hereafter referred to as "WRF-LAI") was adapted from the monthly LAI dataset in WRF-CLM (Subin et al., 2011), which is a function of 16 different PFTs defined in CLM 3.5 and does not vary geographically to match specific location (i.e., each of the 16 PFTs always has the same LAI, irrespective of the latitude and longitude), though it does vary seasonally.

The climatology LAI dataset (hereafter referred to as "CLM-LAI") was from the monthly LAI dataset used in CESM. Unlike the WRF-LAI, the CLM-LAI varies with geographical location, so that the same PFT for the same month, at two different latitudes and longitudes, can have different LAIs. As a result, the differences between WRF-LAI and CLM-LAI at the same geographical location will highlight the effects of spatial biogeographical sensitivity for relatively static LAI datasets. CLM-LAI was originally derived from the MODIS satellite measurements based on Myneni et al. (2002) using the de-aggregation methods described in Lawrence and Chase (2007). The MODIS LAI products observed from 2000 to 2003 were used to determine the monthly LAI patterns for the PFTs defined in CLM, and only the highest quality LAI data (Myneni et al., 2003) were included in this process, except when a month or longer duration of a data gap occurred, then the next highest quality level data were used (Lawrence and Chase, 2007). A more detailed description about the LAI mapping technique can be found in Lawrence and Chase (2007).

For the time-varying LAI dataset (hereafter referred to as "MODIS-LAI"), we used the MODIS Collection 5 LAI (MYD15A2) data at the locations of the six AmeriFlux sites from 2000 to 2006, although similar products can be found in LAI3g (Zhu et al., 2013), GLASS LAI (Xiao et al., 2013), and VIIRS LAI (Xiao et al., 2016). This product (MYD15A2) is derived from the MODIS LAI and a Fractional Photosynthetically Active Radiation (FPAR) algorithm based on a three dimensional radiation transfer theory (Myneni et al., 2002), and developed for inversion using a look-up table approach (Knyazikhin et al., 1998a,b; Privette et al., 2002) to form the 8-day composite results that covers a 7 km by 7 km area of the sites with 1 km resolution. The back-up algorithm is triggered to estimate LAI and FPAR using vegetation indices when the main algorithm fails (Myneni et al., 2003). The product also includes extensive quality control information regarding cloud, saturation and geometry conditions, and only the highest quality LAI data (Myneni et al., 2003) derived from the main algorithm were selected to represent the MODIS-LAI. In cases where the highest quality LAI (Myneni et al., 2003) was not available for all the 7 km by 7 km area of the sites, the MODIS-LAI was interpolated from the highest quality LAI recorded before and after 2 time steps.

The effect of spatial heterogeneity within the 7 km by 7 km area of the sites in the MODIS-LAI was examined by comparing the MODIS-LAI series derived from the 7 km by 7 km area of the sites and the MODIS-LAI series derived at the location of the sites (1 km by 1 km pixel) (SM1). The results show that LAI directly derived at the location of the sites generally agrees with the areal mean MODIS-LAI with the use of the main algorithm (Myneni et al., 2003), but it deviates significantly from the areal mean MODIS-LAI with the use of the back-up algorithm (Myneni et al., 2003). This result suggests that the selection of signal retrieval algorithm could be more sensitive in MODIS-LAI derivation than spatial heterogeneity. Future studies should be aware of the sensitivity of satellite signal retrieval algorithm, in addition to satellite spatial resolution, when applying satellite-derived LAI to site level scale.

3. Numerical models and experiment design

Two land surface models (LSMs) were used in this study to investigate canopy profile sensitivity, both structural and functional, to biogeophysical and biogeochemical simulations. The first model is the Advanced Canopy-Atmosphere-Soil Algorithm (ACASA), which is a multiple canopy layer model. The ACASA model includes detailed plant physiology and turbulence transport within and above vegetation canopies. The second model is the Noah Land Surface Model (Noah LSM), which is a single canopy layer model. The Noah LSM applies relatively simple parameterizations to estimate the bulk effects from a series of canopy processes.

3.1. ACASA and its improvement

The ACASA model was developed at the University of California, Davis (Pyles et al., 2000). Based on the diabatic, third order closure method developed by Meyers and Paw U (1986; 1987), the standard version of ACASA has 20 vertical canopy layers to represent the realistic turbulent fluxes of momentum, heat, moisture and carbon dioxide above and within the simulated canopy at half-hourly to hourly time steps; the number of layers can be increased or decreased. The employment of the third order closure method enables ACASA to simulate non-local and counter-gradient turbulent transports in the canopy air space, and realistic simulation results for the vertical profiles in the canopy were reported in Pyles et al. (2000; 2004). A near-exact quartic energy balance formulation coupled with a spherical leaf distribution assumption has been used to enable ACASA to calculate surface temperature accurately especially in situations where surface temperatures in the canopy differ significantly from ambient air temperature (Paw U and Gao, 1988). The average leaf and stem temperatures within each vertical layer are obtained by performing a weighted average of the shaded and sunlit leaves and stem temperatures within a layer, although the leaf and stem surface temperatures for each of the nine sunlit leaf angle classes and one shaded leaf angle class are simulated individually for each layer.

In addition to the biogeophysical processes listed above, ACASA can also simulate plant physiological responses to changes in micro environmental conditions based on the coupled equation set formed by the Ball-Berry stomatal conductance (Leuning 1990; Collatz et al., 1991) and the Farquhar and von Caemmerer (1982) photosynthesis equations described in Su et al. (1996). A schematic diagram for these processes is shown in Fig. 1. Besides the stand-alone version of ACASA, ACASA can also be coupled with regional scale atmospheric models like the Fifth Generation PSU/NCAR Mesoscale Model (MM5) (Pyles et al., 2003) and the Weather Research and Forecasting (WRF) model (Falk et al., 2014; Xu et al., 2014).

The ACASA model used in this study differed from its predecessor (Pyles et al., 2000) in multiple ways, including: (a) The evapotranspiration processes were improved through adjusting the amount of canopy water based on the principle of mass conservation, and adapting the soil water moisture effects on bare ground evaporation consistent with version 4.5 of the Community Land Model (CLM 4.5) (Oleson et al., 2013). (b) A more general plant root distribution formula that accounts for 16 different PFTs adapted from CLM 4.5 (Oleson et al., 2013) was applied in this version of ACASA. (c) The accuracy of upscaling carbon assimilation from sunlit and shaded leaf classes to the entire canopy was improved by correcting the weighting factor for individual leaf angle classes.

The ACASA model is driven by time information and eight meteorological variables at half-hourly to hourly time intervals, which are specific humidity, precipitation, downwelling shortwave radiation, downwelling longwave radiation, air temperature, air pressure, wind speed, and carbon dioxide concentration, above the canopy. These model input variables were provided by site measurements directly taken at the six AmeriFlux sites (Table 1) from years 2000 to 2006. The ACASA model simulates steady state turbulence characteristics at half-hourly to hourly time steps through the iterative approach described in Pyles et al. (2000), and no initial spin-up time is required by the model.

3.2. Noah land surface model

The single canopy layer Noah land surface model (Noah LSM) was developed through multi-institutional cooperation, and it has been widely applied in operational weather and climate predictions supported by National Centers for Environmental Prediction (NCEP) (Mitchell et al., 2005). A more detailed description of model heritage and model parameterizations can be found in Chen and Dudhia (2001) and Ek et al. (2003).

The offline one dimensional Noah LSM version 3.4.1 was used in this study, which has four soil layers (with depths of 0.1 m, 0.3 m, 0.6 m, and 1.0 m) and a single canopy layer (Mitchell et al., 2005). The vegetation types and plant morphological parameters are defined based on land-use categories assigned from U.S. Geological Survey (USGS)

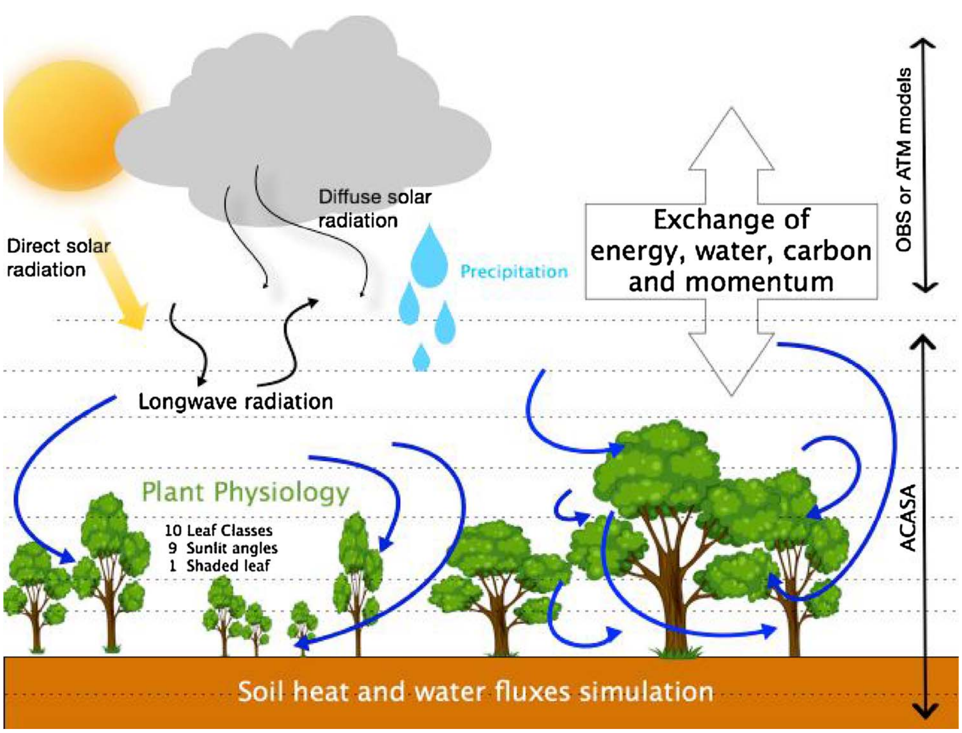

Fig. 1. Schematic diagram for the ACASA model. The necessary inputs can be obtained from observations or atmospheric models. The multiple canopy layer feature in ACASA enables it to realistically capture local and non-local turbulence transport fluxes from the surface layer and heat and water fluxes from the soil layer.

database. The soil types and parameters are defined by the Food and Agriculture Organization (FAO) database. Model source code and parameter tables can be downloaded from Noah LSM website (http://www.ral.ucar.edu/research/land/technology/lsm.php).

The Noah LSM is driven by time information and eight meteorological variables at half-hourly to hourly time intervals, which are wind speed, wind direction, air temperature, downwelling shortwave radiation, downwelling longwave radiation, precipitation, air pressure, and relative humidity. These model input variables were provided by site measurements directly taken at the six AmeriFlux sites (Table 1) from years 2000 to 2006.

3.3. Experimental design

Two sets of simulations at six AmeriFlux sites from 1 January 2000 to 31 December 2006 were conducted using each of two LSMs (i.e., ACASA and Noah) to test our two hypotheses. All simulations at each AmeriFlux site were driven by the meteorological conditions collected from the AmeriFlux network with varying realism of ecological conditions represented by three different LAIs: MODIS-LAI, WRF-LAI and CLM-LAI. The inter-comparison between LAI datasets and land surface models aims to (1) identify the most critical component in a LAI dataset, (2) evaluate model performance associated with simple and sophisticated model physics, and (3) diagnose the sensitivity of canopy structural representation shown in different model configurations.

Two additional sets of simulations were conducted to examine and evaluate the effects of different structural and functional treatments in canopy profiles. The first set of simulations, ACASA_SL, was designed to resemble single layer canopy representation under the model configuration used in ACASA, where all active leaves were placed at the top of the canopy and all scalar profiles (air temperature, specific humidity and CO2 concentration) were kept vertically invariant, set equal to measurements given at the top of the simulated canopy (Section 3.1). The ACASA_SL run was used to analyze model sensitivity to single and multiple layer representation of canopy structure with the same plant physiology and turbulence closure scheme. The second set of simulations, ACASA_CP, was designed to examine the importance of another aspect of ACASA. In ACASA_CP, everything was the same as ACASA except the use of vertically invariant scalar profiles throughout the simulated canopy. Thus, the ACASA_CP run was used to examine the importance of vertical scalar profiles and the potential of the profiles to cause physiological feedback to canopy carbon and water fluxes. Both ACASA_SL and ACASA_CP were driven with the same MODIS-LAI and meteorological conditions taken at the six AmeriFlux sites.

Filling missing data that were required for model inputs was performed in order to conduct continuous model simulation throughout the years 2000–2006. For blocks of less than 2 h of missing data, a linear interpolation method was used to fill in gaps with neighboring measurements. Larger blocks of missing data were filled with typical values of the same time window calculated from the measurements taken at that week (or month, if the measurements of the entire week were missing). However, all of the simulation results driven by gap filled data were excluded for the model evaluation presented here to avoid potential biases caused by unreliable model inputs.

All of the simulation results were compared with field measurements gathered at the six AmeriFlux sites after applying the quality control criteria described in Section 2.1. The model outputs (i.e., energy and carbon fluxes) from each set of simulations were examined using the two tailed Student's t-test, and the t-tests suggested that the differences in model outputs are statistically significant between each of the individual simulations with p-values less than 0.05 (results not shown). The major differences among each set of simulations were summarized in Table 2.

4. Results and discussion

4.1. Seasonal natural variability in LAI

To discuss canopy structural impacts on biogeophysical and biogeochemical simulations, we first compared the variation patterns among different LAI datasets. The time evolution of the MODIS-LAI, the CLM-LAI and the WRF-LAI at the six AmeriFlux sites from 2000 to 2006 are shown in Fig. 2. The corresponding ground-based LAI measurements recorded in the AmeriFlux Biological, Ancillary, Disturbance and Metadata (BADM) dataset (Law et al., 2008) were also plotted in Fig. 2 to represent the ground truth conditions. The length of the growing season depicted by the MODIS-LAI can be roughly captured by the WRF-LAI at the forest sites, although the monthly variation patterns and values are significantly different between these two datasets except for the deciduous broadleaf forest site (Fig. 2). Moreover, WRF-LAI failed to capture both the growing season length and the monthly variation patterns at the C3 grassland site, and most of the growing seasons depicted in the MODIS-LAI were represented as senescent periods in the WRF-LAI. On the other hand, the CLM-LAI varies coherently with the MODIS-LAI at all the six AmeriFlux sites, although the CLM-LAI sometimes exhibits larger amount of LAI than those recorded in the MODIS-LAI. Overall, the results show that the CLM-LAI can represent LAI variation features comparable to the MODIS-LAI over the study period, suggesting that monthly LAI dataset with proper geographical (latitude and longitude) sensitivity can be as reliable as time varying LAI dataset with finer temporal resolution.

In general, the WRF-LAI represents canopy leaf evolution reasonably well at the forest sites, where the mean LAI values are higher and the seasonal LAI variations are relatively smaller as compared to the C3 grassland site. The correlation coefficient between the WRF-LAI and the MODIS-LAI can reach up to 0.739 at the forest sites, but they are only weakly anti-correlated to each other (-0.202) at the C3 grassland site. In terms of the amount of LAI, the WRF-LAI presents higher LAI values for all the evergreen needleleaf forest sites than the MODIS-LAI, which could induce stronger evapotranspiration and carbon sequestration with simulations driven by the WRF-LAI. This scenario reverses at the C3 grassland site. Besides, there is a consistent time lag between the growing seasons suggested by the WRF-LAI and those depicted by the MODIS-LAI at USVar, which could contribute to a significant source of simulation errors when applying to canopy structural description.

The CLM-LAI, on the other hand, exhibits similar LAI biases found in the WRF-LAI for the forest sites except for the USBlo site. As a result, land surface simulations over forests driven by the CLM-LAI dataset should have similar behaviors to those generated by the WRF-LAI as discussed above. However, the LAI variation patterns at the C3 grassland site are reasonably captured by the CLM-LAI, and the seasonal time lag issues exhibited in the WRF-LAI can be significantly improved with the inclusion of geographical variations (sensitive to latitude and longitude). The correlation coefficients between the CLM-LAI and the MODIS-LAI can reach up to 0.889 for the forest sites and 0.772 for the C3 grassland site. Therefore, the results show that geographical variations are crucial to relatively static LAI datasets, and the purely PFT dependent LAI dataset (WRF-LAI) may not be able to reasonably represent time-varying LAI phenology.

When compared with ground-based LAI measurements, our results show that MODIS-LAI and CLM-LAI can reasonably capture the observed seasonal LAI variations at USHa1 and USVar, suggesting that phenological changes in LAI can be represented with temporal resolution no coarser than a month. Our results also indicate that MODIS-LAI underestimates site level LAI due to satellite signal saturation (Anav et al., 2013; Murray-Tortarolo et al., 2013) when ground-based LAI measurements are higher than $4\,m^2/m^2$ (Fig. 2). The minimum LAI correction applied in CLM-LAI (Lawrence and Chase 2007) could improve the low LAI bias found in MODIS-LAI at dense evergreen forests (Fig. 2).

Table 2
Description of different model configurations used in this study.

	ACASA	Noah LSM	ACASA_SL	ACASA_CP
Leaf angle class	9 sunlit and 1 shaded on each canopy layer	single leaf class	9 sunlit and 1 shaded on each canopy layer	9 sunlit and 1 shaded on each canopy layer
Model canopy layer	10 layers (adjustable)	single canopy	10 layers (adjustable)	10 layers (adjustable)
Canopy structural description	total LAI interpolated to 10 canopy layers	single layer total LAI	single layer total LAI at the top of the canopy	total LAI interpolated to 10 canopy layers
Scalar fluxes treatment inside canopy	realistic profiles (diagnosed)	NA	constant profiles throughout canopy	constant profiles throughout canopy
Plant physiology	Modified Farquhar and von Caemmerer (Su et al., 1996)	NA	Modified Farquhar and von Caemmerer (Su et al., 1996)	Modified Farquhar and von Caemmere (Su et al., 1996)

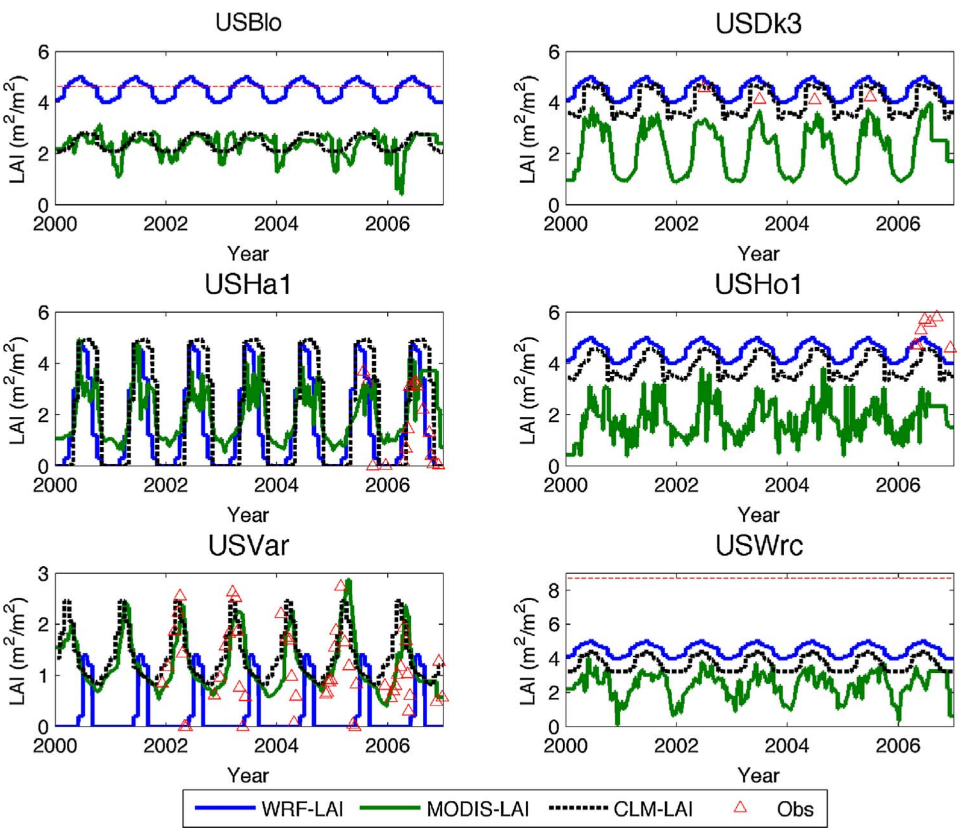

Fig. 2. The Leaf Area Index (LAI) variation from 2000 to 2006 for the six AmeriFlux eddy covariance sites. The names of each site are shown in the abbreviations on top of each figure. Blue lines are the time series for the WRF-LAI, black dash lines are the time series for the CLM-LAI, green lines are the time series for the MODIS-LAI, red triangles are the LAI site measurements, and red dash lines are the LAI suggested in the AmeriFlux BADM dataset. (For interpretation of the references to colour in this figure legend, the reader is referred to the web version of this article.)

4.2. Multiple canopy layer model sensitivity to LAI descriptions

To investigate the impacts of LAI descriptions on a higher order closure multiple canopy layer model, we analyzed the sensitivity in the simulated sensible heat flux, latent heat flux and Net Ecosystem Exchange (NEE) when ACASA was driven by different LAI datasets. Some of the statistical measures for the results simulated by ACASA with the MODIS-LAI, CLM-LAI and WRF-LAI at the six AmeriFlux sites are listed in Table 3. The R squared values and the root mean square errors are generally improved after applying the more realistic MODIS-LAI, and the use of CLM-LAI is able to reproduce reasonable land surface simulations as accurately as the results driven by the MODIS-LAI. The simulations driven by the WRF-LAI, on the other hand, usually exhibit lower R squared values and larger root mean square errors. This shows more realistic, biogeographically sensitive ecological datasets improve the simulation accuracy, meaning that ecological datasets based on static vegetation distributions must be used with caution.

The effects of different canopy structure descriptions on land surface simulations were studied by comparing the differences in the simulated biogeophysical and biogeochemical patterns when ACASA was driven by WRF-LAI and MODIS-LAI, respectively. These two sets of simulations were only different in vertical canopy structural description, as illustrated in Section 3.3. For the sake of brevity, we only present the simulation results obtained at USBlo and USVar, since WRF-LAI and MODIS-LAI deviate the most from each other at these sites (Fig. 2).

The scatter plots between the observed and the simulated energy and carbon fluxes at USBlo show that the simulated latent heat flux tends to be stronger when ACASA is driven by WRF-LAI instead of MODIS-LAI (Fig. 3). This is because the amount of active leaves in WRF-LAI is consistently higher than those in MODIS-LAI (Fig. 2), which strengthens the simulated evapotranspiration and latent heat flux. The simulated sensible heat flux, on the other hand, presents the opposite behavior to the simulated latent heat flux, because energy conservation is strictly guaranteed in ACASA. The simulated NEE tracks the simulated latent heat flux, such that carbon sequestration strength would also be enhanced by the higher LAI described in the WRF-LAI. The results suggest that both LAI datasets can be used to simulate reasonable sensible and latent heat fluxes at USBlo, and the NEE simulation is more sensitive to vertical canopy structure than the energy fluxes simulation. This asymmetric sensitivity can be caused by the non-linear interactions between canopy structure, turbulent characteristics and plant physiological processes in the multiple canopy layer higher order

Table 3
The slope of the linear regression lines (Slope), R squared values (R^2) and root mean square errors (RMSE) for sensible heat (H), latent heat (LE) and NEE simulated by ACASA at the six AmeriFlux sites. The RMSE units for sensible and latent heat fluxes are W m^{-2}, and the RMSE units for NEE are g C m^{-2} s^{-1}.

	H			LE			NEE		
	CLM-LAI	WRF-LAI	MODIS-LAI	CLM-LAI	WRF-LAI	MODIS-LAI	CLM-LAI	WRF-LAI	MODIS-LAI
(a) Slope									
USBlo	0.9024	0.8250	0.9154	0.7837	0.8505	0.7596	1.0228	1.4291	1.0032
USDk3	0.8144	0.8142	0.9330	0.9553	0.9531	0.9044	0.4743	0.4975	0.3693
USHa1	0.9637	1.0162	0.7661	0.8617	0.8429	0.8073	0.6623	0.5355	0.4942
USHo1	0.8735	0.8699	0. 9342	1.0545	1.0479	1.0171	0.8852	0.9292	0.6738
USVar	0.8504	0.7212	0.8456	0.5621	0.1384	0.6037	0.7504	−0.0455	0.7420
USWrc	0.7181	0.7249	0.7514	1.0463	1.0339	1.0288	0.7881	0.8621	0.6499
(b) R^2									
USBlo	0.7520	0.7428	0.7483	0.6896	0.6833	0.6802	0.7027	0.6987	0.6974
USDk3	0.7508	0.7534	0.7590	0.7896	0.7909	0.7966	0.4562	0.4434	0.4748
USHa1	0.6056	0.6155	0.7023	0.6918	0.6644	0.7361	0.7111	0.6463	0.5581
USHo1	0.8118	0.8165	0.8116	0.7544	0.7564	0.7433	0.5962	0.5671	0.6325
USVar	0.7901	0.5980	0.8004	0.5893	0.0625	0.5936	0.5781	0.0184	0.6138
USWrc	0.7869	0.7887	0.7648	0.4988	0.4977	0.4782	0.4362	0.4392	0.4221
(c) RMSE									
USBlo	60.56	57.77	62.18	54.66	60.84	54.31	4.77E-05	7.51E-05	4.69E-05
USDk3	47.78	47.60	69.32	59.86	59.33	55.53	9.06E-05	9.25E-05	8.99E-05
USHa1	92.75	95.50	66.29	58.14	61.13	51.15	5.19E-05	5.82E-05	6.53E-05
USHo1	56.96	56.23	56.93	66.62	65.68	61.41	6.38E-05	6.93E-05	4.95E-05
USVar	54.43	74.47	52.39	61.64	76.37	59.48	5.19E-05	6.02E-05	4.83E-05
USWrc	83.91	83.24	77.66	90.27	88.94	92.35	8.86E-05	9.49E-05	7.86E-05

closure ACASA model.

The effects of different canopy structure descriptions, driven by different LAI datasets, on surface layer simulations shown at USBlo (and all the other forest sites) are relatively straightforward because the WRF-LAI can generally represent the broad picture of the LAI variations at the forest sites (Fig. 2). On the other hand, the WRF-LAI failed to represent reasonable LAI patterns at USVar, a C3 grassland site, in terms of both the magnitude of LAI and the onset time of the growing seasons (Fig. 2), so the simulation results there should reveal more insights of the model sensitivity to canopy structural description. As shown in Fig. 4, there is a bifurcation pattern in the simulated energy fluxes driven by the WRF-LAI, which overestimates sensible and latent heat fluxes when the observed values are relatively weak and vice versa. This is because the actual growing seasons at USVar are spuriously depicted by the WRF-LAI, causing underestimates of latent heat flux during growing seasons and overestimates of latent heat flux during senescent seasons. The simulated energy fluxes can be significantly improved with the use of MODIS-LAI, highlighting the importance of selecting a realistic ecological dataset in land surface simulation. For the carbon flux simulations performed at USVar, it is clear that the simulation driven by the WRF-LAI has difficulty representing reasonable NEE patterns, and this issue can be resolved by applying the more realistic MODIS-LAI to ACASA (Fig. 4). These results suggest that the use of WRF-LAI would not only increase errors in energy and carbon flux simulation, but also lead models to misinterpret land surface processes even with correct model physics. Both types of errors can be avoided by applying more realistic LAI datasets, such as the MODIS-LAI and the CLM-LAI (Table 3), reinforcing that proper phenology and vegetation distribution patterns are necessary for reasonable land surface simulation. Moreover, the results at USBlo and USVar both suggest that NEE simulation is more sensitive to LAI description than sensible and latent heat fluxes simulation, as shown by the use of multiple canopy layer higher order closure ACASA model.

In addition to comparing the scatter patterns of the simulated energy and carbon fluxes at each half hourly interval, we also examined the diurnal cycle patterns calculated from averaging the corresponding half hourly simulation results from years 2000 to 2006. The results for a sample site, USBlo, show that ACASA can simulate reasonable diurnal cycles with all of the LAI datasets (Fig. 5), suggesting that biogeophysical processes are the dominant factors in reproducing diurnal cycles. However, it is clear that the simulated evapotranspiration and carbon sequestration strengths in the simulated canopy are systematically stronger when ACASA is driven by the WRF-LAI rather than by the MODIS-LAI. These biases stem from the higher amount of leaves described in the WRF-LAI, which enhances the simulated evapotranspiration and carbon sequestration strengths. Besides the biases for the mean states, we also noticed that the magnitudes of the deviation between the simulated fluxes driven by WRF-LAI and MODIS-LAI vary significantly throughout a day, indicating that processes with shorter time scales controlled by radiation and turbulence schemes are as important as the reliability of the slowly varying ecological conditions used in land surface models. Similar biases can be found between the results driven by the CLM-LAI and the MODIS-LAI, although the differences are much smaller than those discussed above.

4.3. Single canopy layer model sensitivity to LAI descriptions

The sensitivity to different canopy structure descriptions simulated by a single canopy layer model was investigated by analyzing the simulation results from Noah LSM driven by different LAI datasets. Some of the statistical measures for the simulation results from Noah LSM driven by the MODIS-LAI, CLM-LAI and WRF-LAI at the six AmeriFlux sites are summarized in Table 4. The results show that, when driven by the same LAI dataset, simulations done at evergreen forest sites, which generally have more muted seasonal and intraseasonal variability, usually agree reasonably with field measurements while simulations done at sites with more prominent seasonal variations in LAI generally exhibit lower R squared values and higher root mean square errors. The Noah LSM results also poorly simulated the complex ancient temperate rainforest (USWrc), which could be due to the strong seasonality of precipitation at the site coupled with vertical complexity of the canopy. The model performance could be improved by introducing model parameters that better describe the investigated sites through a series of model tuning experiments. The weakness found at sites with stronger seasonality in canopy structural temporal variations may arise from the fact that the single canopy layer representation used in Noah LSM is not sufficient to represent the comprehensive processes between the soil surface and vegetation canopy (Niu et al., 2011; Yin et al., 2016). This

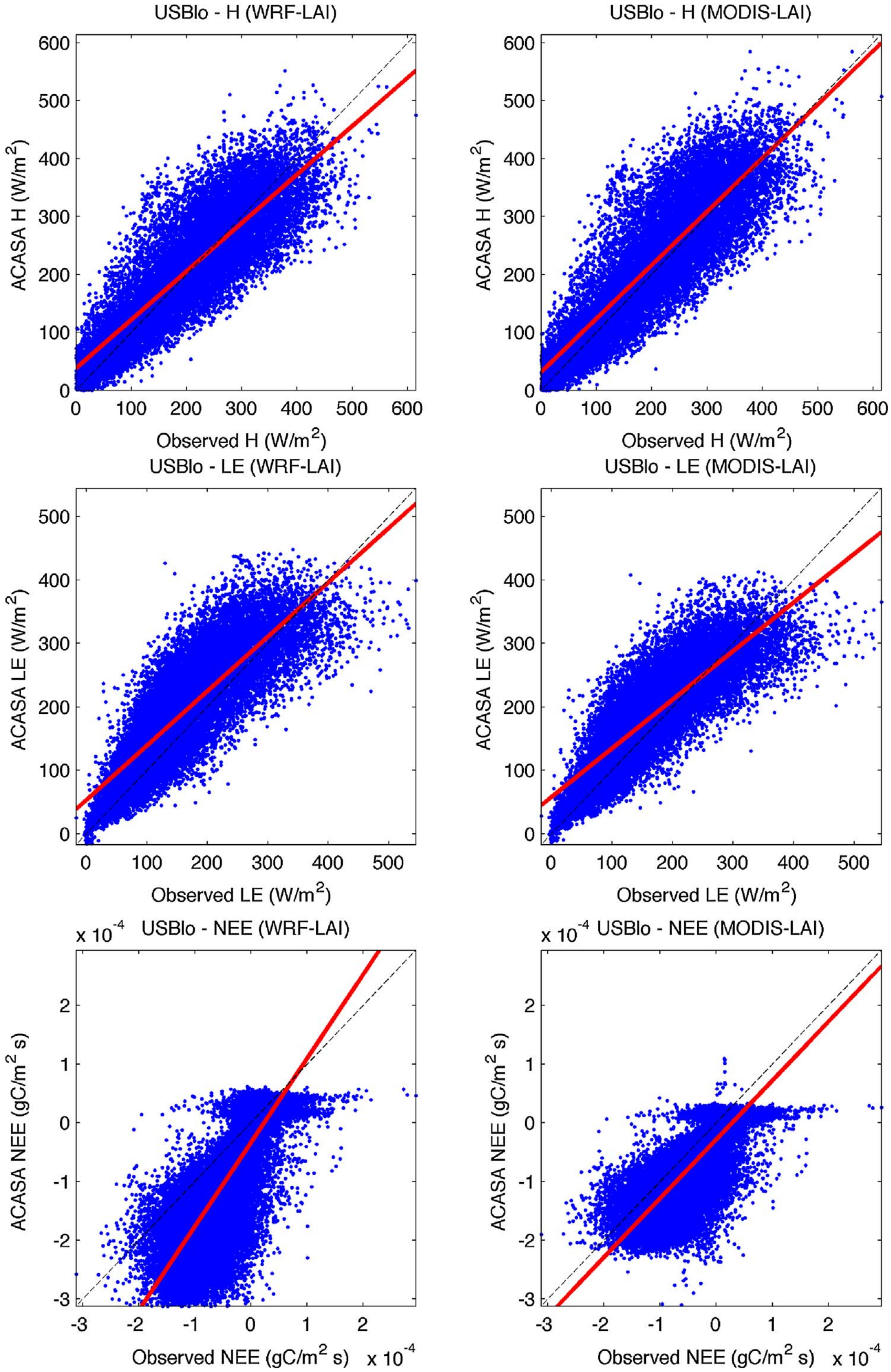

Fig. 3. Scatter plots between half hourly observed and simulated sensible heat flux (H), latent heat flux (LE) and Net Ecosystem Exchange (NEE) at USBlo from years 2000 to 2006. Red lines are linear regression lines and black dashed lines show the one to one relationship in each plot. The simulated results are from ACASA driven by the WRF-LAI and the MODIS-LAI.

result thus suggests that Noah LSM can be a useful tool reproducing general land surface patterns for large-scale climate simulations, but it needs to be used with caution for fine scale terrestrial interaction simulations. Similar to the results shown in Section 4.2, the root mean square errors generally reduce with the use of the MODIS-LAI.

The scatter plots of the energy fluxes measured by the AmeriFlux network and those simulated by Noah LSM driven by the WRF-LAI and MODIS-LAI at USBlo and USVar are shown in Fig. 6. For USBlo, Noah LSM successfully simulates reasonable sensible and latent heat fluxes with both LAI datasets. Similar to the results simulated by ACASA (Fig. 3), latent heat flux simulated by Noah LSM tends to be higher with the use of the WRF-LAI, suggesting that canopy structural impacts are consistent across different model configurations and levels of complexity. For USVar, Noah LSM significantly underestimates sensible heat flux and exhibits a clear bifurcation pattern for the simulated latent heat flux with both LAI datasets. The reason for the unsatisfactory latent heat flux simulation with the use of the WRF-LAI is primarily driven by the inappropriate phenological and morphological descriptions in the WRF-LAI (Section 4.1), which spuriously prescribes the amount of active leaves performing evapotranspiration during senescent seasons and vice versa. The simulation results can be slightly improved with the use of MODIS-LAI, although the bifurcation pattern

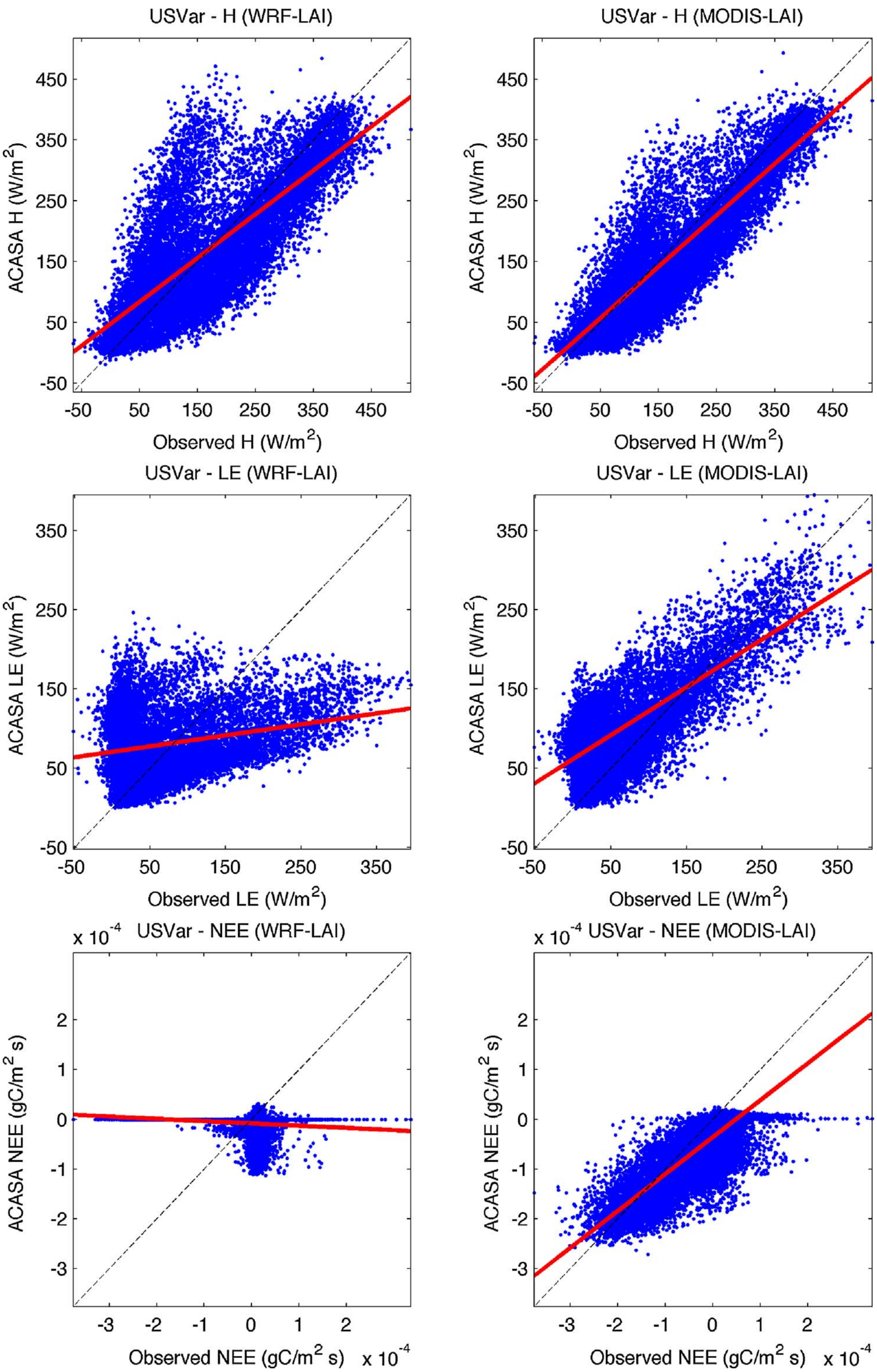

Fig. 4. Same as Fig. 3, but for USVar.

shown in the latent heat flux simulation remains. The main reason for the limited improvement is that Noah LSM exaggerates plant transpiration during the transition period from growing season to senescent season, and this deficiency in plant transpiration modeling prevents further improvements in the results, even with more reliable canopy structural description.

4.4. Sensitivity to model complexity

As shown in Sections 4.2 and 4.3, simulation results from ACASA and Noah LSM not only present differences in model performance, but also exhibit contrasting sensitivity to canopy structural description. When driven by the same LAI dataset, ACASA generally performs better than Noah LSM with lower root mean square errors for the simulated energy fluxes, suggesting that a more sophisticated multiple canopy layer higher order closure model has advantages in land surface simulation. When the same model is applied, the use of MODIS-LAI can effectively improve latent heat flux simulation facilitated by its time-varying dynamical variation feature, confirming that a more realistic time-varying ecological dataset is critical to portraying ecosystem

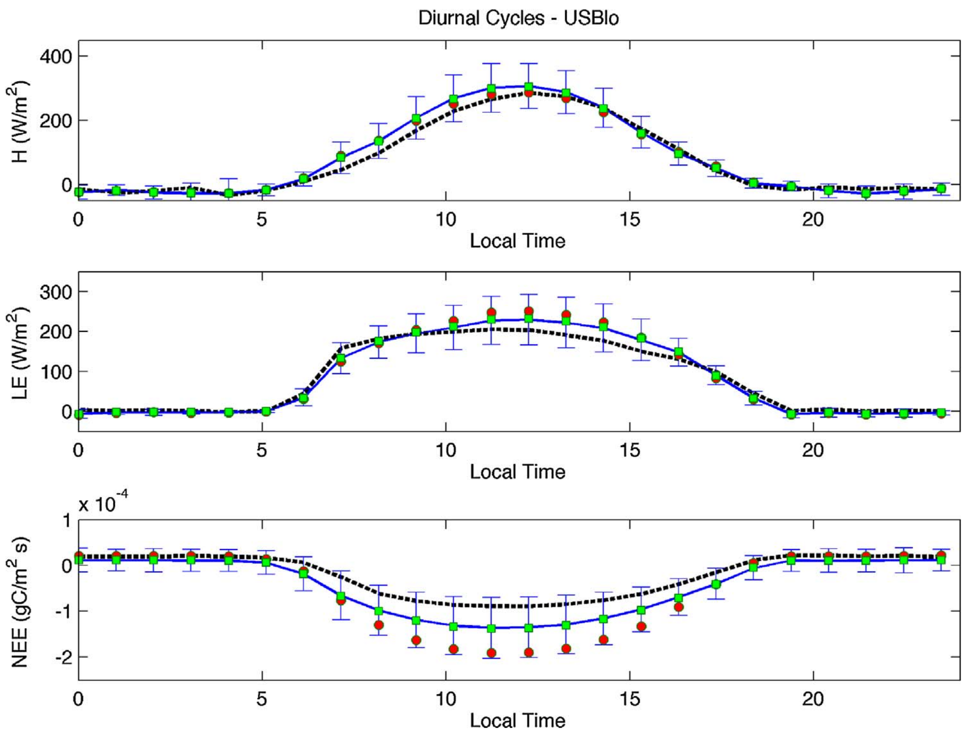

Fig. 5. Mean diurnal cycles for sensible heat flux (H), latent heat flux (LE) and NEE at USBlo, averaged from years 2000 to 2006. Red dots are the simulation results for the WRF-LAI, green squares are the simulation results for the CLM-LAI, blue lines are the simulation results for the MODIS-LAI, and the black dashed lines are the observed diurnal cycles. The error bars are the root mean square errors at each half hour window associated with the simulation results for the MODIS-LAI. (For interpretation of the references to colour in this figure legend, the reader is referred to the web version of this article.)

Table 4
The slope of the linear regression lines (Slope), R squared values (R^2) and root mean square errors (RMSE) for sensible heat (H) and latent heat (LE) simulated by Noah LSM at the six AmeriFlux sites. The RMSE units for sensible and latent heat fluxes are $W\,m^{-2}$.

	H			LE		
	CLM-LAI	WRF-LAI	MODIS-LAI	CLM-LAI	WRF-LAI	MODIS-LAI
(a) Slope						
USBlo	0.7632	0.7298	0.7673	0.8984	1.0888	0.8717
USDk3	0.5696	0.5656	0.6028	0.9106	0.9173	0.8444
USHa1	0.2641	0.2680	0.2693	0.9008	0.8551	0.8372
USHo1	0.6942	0.6879	0.7328	0.9634	0.9741	0.8023
USVar	0.3379	0.3362	0.3399	0.2622	0.0655	0.2723
USWrc	0.4005	0.3816	0.4502	0.8617	0.8886	0.8035
(b) R^2						
USBlo	0.6510	0.6506	0.6499	0.6647	0.6887	0.6631
USDk3	0.6016	0.6008	0.5965	0.7662	0.7665	0.7626
USHa1	0.1889	0.1753	0.1801	0.7362	0.7064	0.7162
USHo1	0.7508	0.7465	0.7726	0.7002	0.7007	0.7077
USVar	0.3856	0.3155	0.3901	0.0422	0.0026	0.0457
USWrc	0.5111	0.4888	0.5826	0.2307	0.2294	0.2464
(c) RMSE						
USBlo	89.26	98.08	88.44	58.22	67.28	57.39
USDk3	76.02	76.55	72.08	60.18	60.44	59.08
USHa1	169.05	166.85	167.09	58.24	58.29	56.91
USHo1	98.46	99.77	87.37	58.54	59.60	47.94
USVar	153.23	150.63	153.07	117.77	123.64	117.20
USWrc	169.18	173.87	157.57	134.59	140.53	119.06

response. Nevertheless, ACASA generally exhibits stronger sensitivity to changes in canopy structural description as compared to Noah LSM. For example, root mean square errors for the latent heat flux simulated by ACASA at USVar is reduced by 22.1% after switching from the WRF-LAI to the MODIS-LAI, but the Noah LSM counterpart only shows a reduction of only 5.2%. The differences in canopy structural sensitivity between multiple and single canopy layer models could be further amplified in carbon flux simulations, since the results shown in Section 4.2 suggest that carbon dioxide exchange is more sensitive than other exchange processes. All of these results suggest that the validity of model physics is equally important to the realistic time variation of canopy structural LAI. Therefore, model inter-comparison studies should include the uncertainty in different canopy structure descriptions such as LAI, in addition to analyzing biases entirely contributed by different model turbulent transfer and layering physics.

4.5. Sensitivity to LAI uncertainty

The fidelity of applying MODIS-LAI at the spatial extent of flux footprints of eddy covariance measurements is examined in this section. Model sensitivity to the uncertainty embedded in MODIS-LAI was investigated at two sample sites, USBlo and USWrc, as the relatively unchanged LAI measured at those sites was greatly underestimated by MODIS-LAI (Fig. 2). The simulation results of ACASA and Noah LSM using ground measured LAI were summarized in SM 2. When ACASA is driven by ground measured LAI, the simulated latent heat flux does not necessarily increase with the increase in LAI, although the simulated carbon uptake does (SM 3). This is because LAI is not directly related to the latent heat flux calculated in ACASA, as energy fluxes are simulated through a set of canopy processes that can be non-linearly affected by changes in LAI. On the other hand, Noah LSM exhibits a more linear dependency with the use of LAI, and the simulated latent heat flux increases with the use of higher LAI suggested by ground measurements (SM 4). Our results show that the simulated fluxes correlate well between the use of MODIS-LAI and ground measured LAI, for both ACASA (SM 3) and Noah LSM (SM 4). Therefore, MODIS-LAI could be a useful tool representing canopy structure for land surface simulation conducted at site level scale, although it may introduce biases due to its underestimation of ground measured LAI.

Our results show that the lower LAI prescribed in MODIS-LAI can lead to underestimation in the simulated NEE, and it has limited effects on the simulated latent heat flux (SM 3). This pattern is consistent to those shown in Section 4.2 that carbon dioxide exchange is more sensitive than other terrestrial exchange processes. Our results thus suggest that time-varying MODIS-LAI can be a useful proxy for ground measured LAI at site level scale, although it could contribute to weaker NEE simulation due to its underestimation bias.

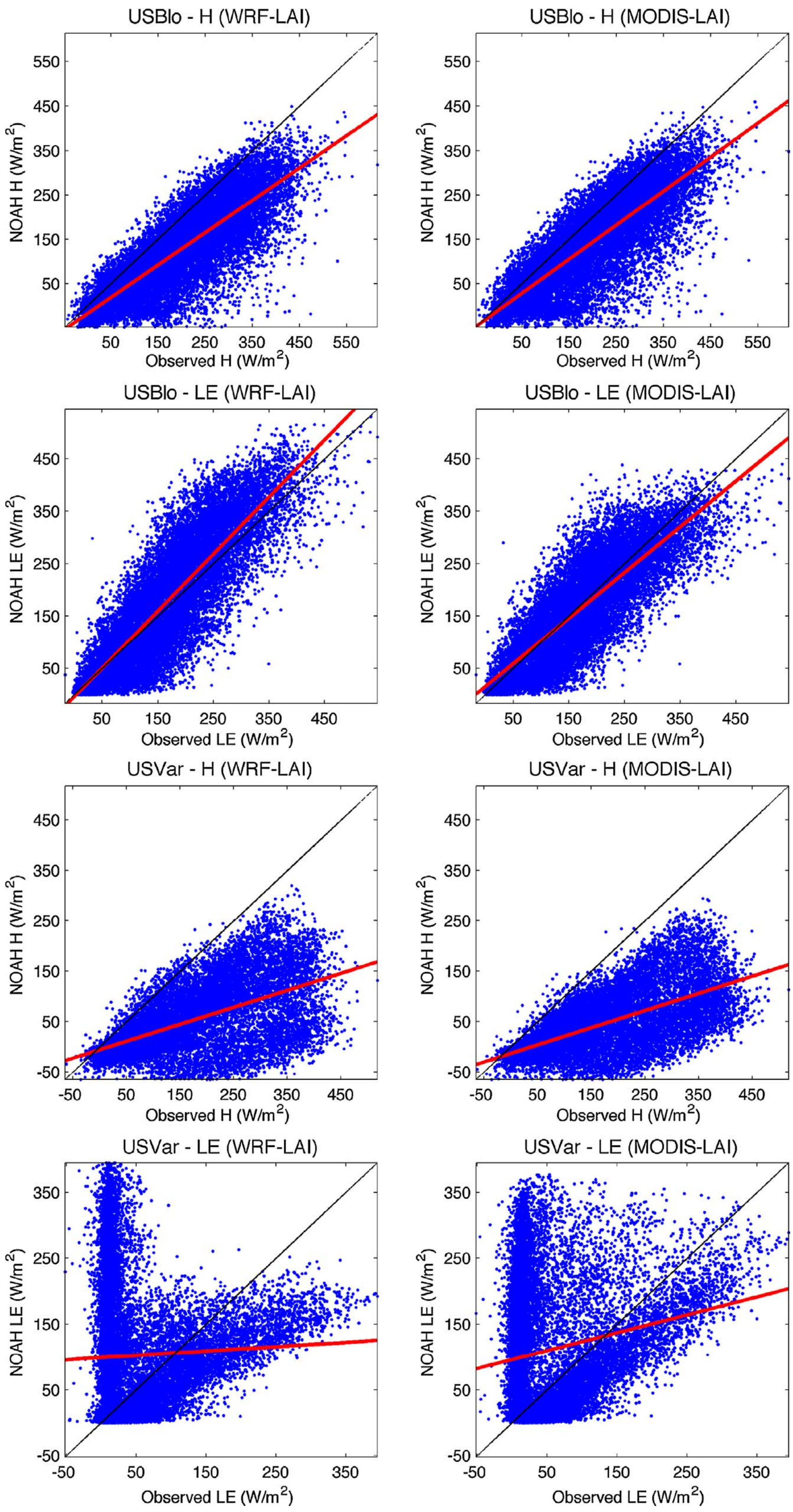

Fig. 6. Scatter plots between half hourly observed and simulated sensible heat flux (H) and latent heat flux (LE) at USBlo and USVar from years 2000 to 2006. Red lines are the linear regression lines and black dashed lines are the one to one line. The simulated results are from Noah LSM driven by the WRF-LAI and the MODIS-LAI.

5. Sensitivity to model physics

The sensitivity of land surface simulation to different approaches in model physics is investigated in this section. To simplify the analysis, the following discussion only includes simulation results driven by the 'best' canopy structure dataset, the time-varying MODIS-LAI, to minimize contributions from other controlling factors.

Table 5
The slope of the linear regression lines (Slope), R squared values (R^2) and root mean square errors (RMSE) for simulated sensible heat (H), latent heat (LE) and NEE from ACASA_SL and ACASA_CP at the six AmeriFlux sites. The RMSE units for sensible and latent heat fluxes are $W\,m^{-2}$, and the RMSE units for NEE are $g\,C\,m^{-2}\,s^{-1}$.

	H		LE		NEE	
	ACASA_SL	ACASA_CP	ACASA_SL	ACASA_CP	ACASA_SL	ACASA_CP
USBlo	1.0461	0.9696	0.6622	0.7287	1.6483	1.1032
USDk3	0.9664	0.9714	0.8241	0.8851	0.8846	0.4433
USHa1	0.7192	0.8023	0.6041	0.7499	1.2946	0.5434
USHo1	0.9446	0. 9768	0.8785	0. 9732	1.2975	0. 7299
USVar	0.7590	0.8672	0.5766	0.4967	1.0071	0.9001
USWrc	0.6413	0.7556	0.7745	0.9945	1.2968	0.6809
USBlo	0.7682	0.7569	0.6909	0.6894	0.6090	0.7041
USDk3	0.7494	0.7581	0.7809	0.7946	0.4285	0.5132
USHa1	0.6868	0.6891	0.6653	0.7273	0.5882	0.5759
USHo1	0.8045	0. 8204	0.6771	0.7398	0.6188	0. 6409
USVar	0.6598	0.7599	0.3374	0.5177	0.6402	0.6237
USWrc	0.6848	0.7901	0.2703	0.4944	0.3973	0.4130
USBlo	80.69	69.06	52.67	50.51	1.22E-04	5.32E-05
USDk3	89.29	80.85	64.24	57.26	1.49E-04	8.62E-05
USHa1	67.14	68.23	63.71	51.57	1.31E-04	6.44E-05
USHo1	57.60	55.58	53.76	55.99	1.04E-04	5.04E-05
USVar	71.98	57.70	86.99	58.28	6.18E-05	5.61E-05
USWrc	91.16	81.90	98.70	85.10	1.76E-04	8.27E-05

5.1. Noah LSM versus the single layer ACASA

Some of the statistical properties derived from the simulation results from the single layered, but still with higher order closure turbulent physics, ACASA_SL, are summarized in Table 5. The results show that ACASA_SL generally outperforms Noah LSM with higher R squared values and lower root mean square errors for the energy fluxes. The major differences between ACASA_SL and Noah LSM are the use of a higher order closure scheme and the inclusion of more advanced plant physiology in the ACASA_SL model (Table 2). Therefore, the edge held in ACASA_SL suggests that the use of more sophisticated ecophysiological and turbulence transfer schemes can better represent ecosystem response to changing micro environmental conditions.

5.2. ACASA_SL versus ACASA_CP

Some of the statistical properties for the energy and carbon fluxes simulated by ACASA_CP, which includes multiple canopy layers but artificially keeps the scalar profiles constant, are summarized in Table 5. The inclusion of this model allows assessment of the importance of multiple canopy layer representation, even when vertical profiles which could result in differential physiological feedback in different layers, are held constant. The results show that ACASA_CP output usually exhibits higher R squared values and lower root mean square errors than ACASA_SL output, suggesting that the inclusion of realistic canopy architecture in model vertical layers (Table 2) improves scalar flux simulations. Therefore, the use of multiple canopy layer models that portray more realistic vertical structural profile is beneficial to land surface simulation.

The mean profiles for daytime and nighttime energy and carbon fluxes and the corresponding state variables at USBlo simulated by ACASA_SL and ACASA_CP for years 2000–2006 are plotted in Figs. 7 and 8, respectively. During daytime, the results show that latent heat flux and NEE simulated by ACASA_SL are significantly stronger than those from ACASA_CP, although both of the models share the same profiles for all the state variables. This difference is primarily driven by the additional portion of leaves allocated at the top of the canopy in ACASA_SL due to its single canopy representation, which increases the amount of radiation energy absorbed and utilized by plant leaf tissues to perform evapotranspiration and photosynthesis. The sensible heat flux simulated by ACASA_SL, on the other hand, is significantly lower than the ACASA_CP counterpart, balancing the higher latent heat flux simulated with the same available energy. During nighttime, condensation warming is stronger with the use of ACASA_SL, resulting in higher vegetation temperature (sensible heat flux) and higher NEE (plant respiration) as compared to the ACASA_CP counterparts. These results suggest that realistic canopy structural representation not only produces reasonable scalar flux profiles (Figs. 7 and 8), but also reduces simulation error caused by overly simplified canopy morphological description (Table 5).

5.3. ACASA_CP versus ACASA

As shown in Tables 3 and 5, the model performance is comparable when both ACASA_CP and ACASA were driven with the MODIS-LAI. However, we found that the simulated sensible heat flux and NEE are stronger (latent heat flux is weaker) with the use of ACASA_CP, which indicates that the lack of realistic vertical profile representation for biometeorological state variables (Table 2) creates systematic biases in land surface simulation. This is because biometeorological state variables vary differently throughout the simulated canopy, and failure to represent those vertical variations misrepresents the detailed ecophysiological response processes inside canopy. The mean vertical profiles for daytime and nighttime energy and carbon fluxes and the corresponding state variables at USBlo simulated by ACASA_CP and ACASA for years 2000–2006 are shown in Figs. 7 and 8, respectively. During daytime, air temperature and specific humidity increase with canopy depth, resulting in weaker sensible heat flux and stronger latent heat flux with the use of ACASA. On the other hand, daytime carbon dioxide concentration decreases with canopy depth, due to the photosynthetic sink inside canopy, resulting in weaker mean NEE simulation in ACASA due to weaker carbon concentration feedbacks. During nighttime, air temperature decreases with canopy depth, resulting in an opposite bias for the simulated sensible heat flux when comparing ACASA and ACASA_CP output. However, the differences between specific humidity profiles are not strong enough to have significant impacts on latent heat flux simulation during nighttime, and both sets of simulations produce similar condensation warming effects inside the canopy. Our results show that daytime energy and carbon fluxes simulated between ACASA and ACASA_CP at USBlo can be quite different inside canopy (Fig. 9), although their momentum fields are about the same, which is not surprising given that ACASA_CP still allowed vertical profiles of wind speed, while fixing only the temperature, humidity, and carbon dioxide profiles. This shows the scalar profiles can vary significantly throughout

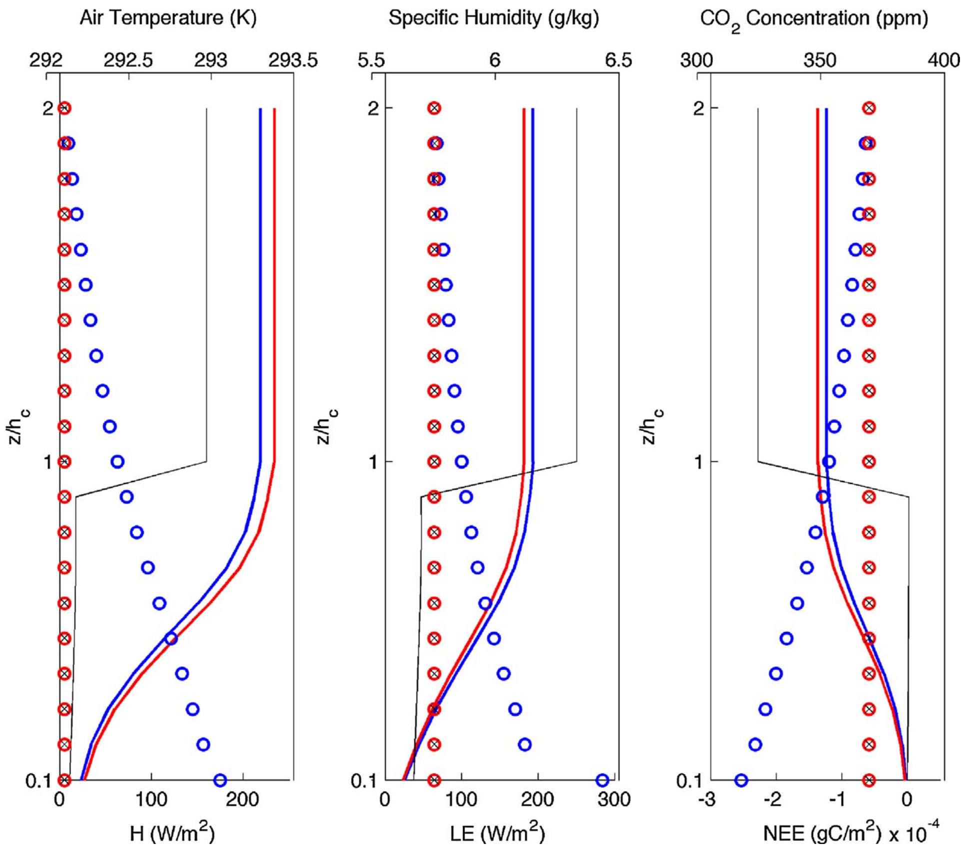

Fig. 7. Solid lines are the mean vertical profiles (bottom axes) for the simulated daytime sensible heat flux (H), latent heat flux (LE) and NEE at USBlo for years 2000–2006. The corresponding scalar profiles (top axes) for the simulated daytime air temperature, specific humidity and carbon dioxide concentration are plotted in open circles (black crosses for ACASA_SL). The results from ACASA, ACASA_SL and ACASA_CP are colored by blue, black and red, respectively. h_c stands for canopy height, and z/h_c is the nondimensional height normalized by canopy height. (For interpretation of the references to colour in this figure legend, the reader is referred to the web version of this article.)

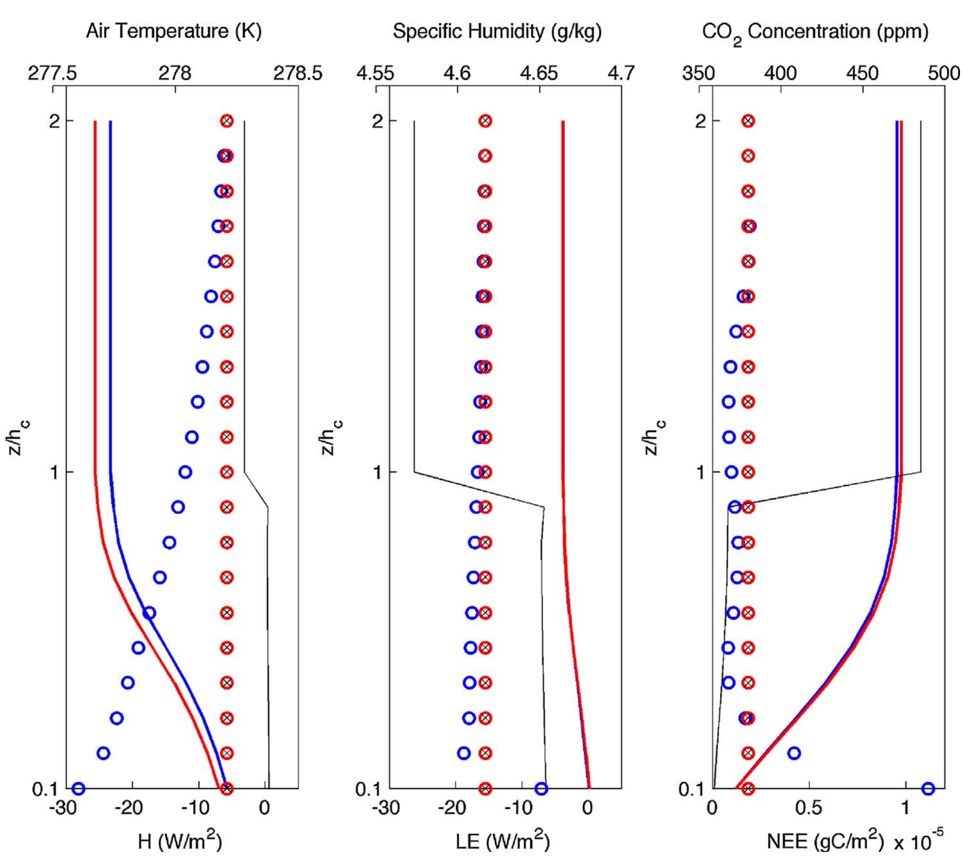

Fig. 8. Same as Fig. 7, but for nighttime.

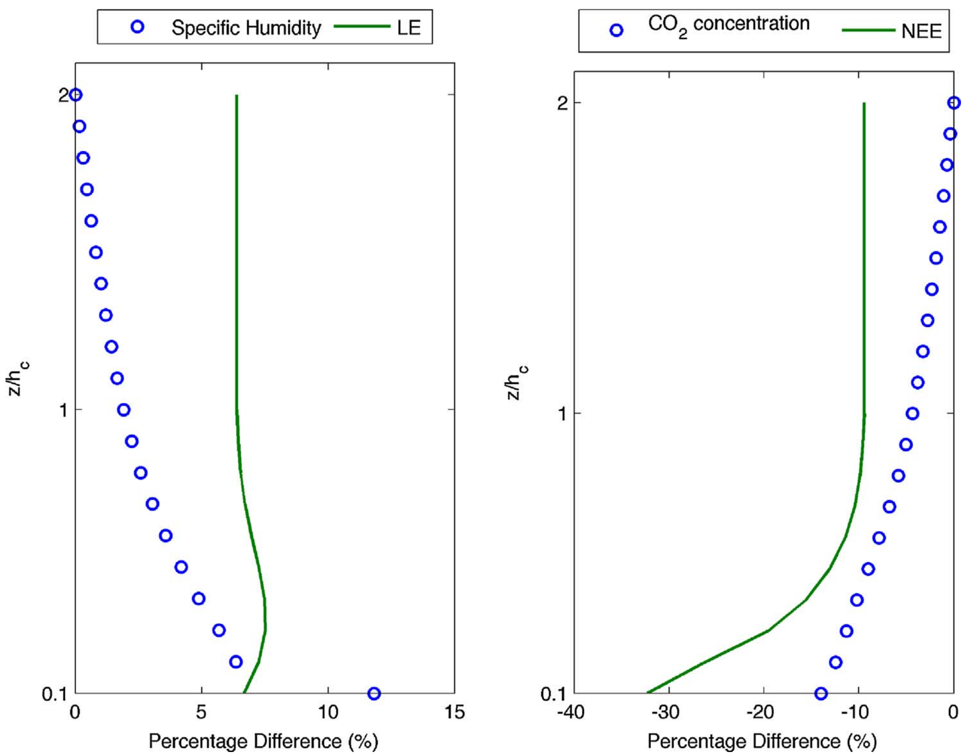

Fig. 9. Percentage difference profiles for the mean daytime scalars (open circles) and fluxes (solid lines) simulated between ACASA and ACASA_CP at USBlo for years 2000–2006. h_c stands for canopy height, and z/h_c is the nondimensional height normalized by canopy height.

canopy, which cause plant physiological process feedback on energy and carbon fluxes. We found that the mean daytime specific humidity can be up to 12% greater, and mean daytime carbon dioxide concentration can to up to 14% lower, with the use of ACASA (Fig. 9). When ACASA_CP is replaced by ACASA, our simulation results at the six AmeriFlux sites indicate that there would be a −6%, 6% and −10% shift in magnitudes for the simulated sensible heat flux, latent heat flux and NEE, respectively. These results establish that the inclusion of realistic treatments for vertical scalar profiles has advantages in properly representing the ecophysiological responses of land surfaces.

6. Conclusions

We conducted a series of LSM simulations for six AmeriFlux sites using the single canopy layer Noah LSM and the multiple canopy layer ACASA to study canopy profile sensitivity on land surface simulations. Some of the concluding remarks are summarized as following:

- The application of a more realistic time-varying LAI dataset improves land surface simulations, which confirms previous studies that LAI is a major factor in land surface simulation. The root mean square errors for the simulated evapotranspiration and NEE are reduced by 10%, and 15%, respectively when using the more realistic time-varying MODIS-LAI instead of WRF-LAI in ACASA. Similar patterns can be found for Noah LSM, although the simulation results are less sensitive to different LAI datasets.
- The MODIS-LAI can be a useful tool representing LAI at site level scale, although its underestimation bias may lead to weaker NEE simulation. Our results indicate that the use of satellite signal retrieval algorithms has significant impacts on the performance of MODIS Collection 5 LAI (MYD15A2), in addition to satellite signal saturation effects documented in the current literature.
- The comparison between energy fluxes simulated by Noah LSM and ACASA suggests that Noah LSM can be almost as accurate as ACASA when seasonal variation in canopy structure is less prominent, but ACASA generally exhibits higher R squared values and lower root mean square errors. When seasonal variation in canopy structure is significant, Noah LSM has difficulty in representing ecosystem response during the transition period from growing season to senescent season while ACASA is still relatively accurate.
- The comparison between ACASA_SL (total LAI placed at the top of the canopy layer) and ACASA_CP (constant scalar profiles throughout the simulated canopy) shows that realistic representation of vertical canopy architecture is beneficial to land surface simulations. Therefore, multiple canopy layer representation should be used to portray the structural profile of the simulated canopy.

All of these findings show that canopy profiles, both in terms of structural and functional, can have significant impacts on land surface simulations through direct effects from canopy structure representation and indirect effects from model turbulence physics parameterization. The use of a land surface model that reasonably represents ecosystem structural and functional responses to microclimate conditions driven by a realistic LAI dataset can thus properly represent surface layer exchange as driven by current and future climate drivers.

Acknowledgments and Data

This research was supported through the National Science Foundation award EF1137306/MIT subaward 5710003122, the National Center of Atmospheric Research computing projectUCDV0007 to the University of California Davis, and the United States Department of Agriculture National Institute of Food and Agriculture, Hatch project CA-D-LAW-4526H and Hatch/Multistate project CA-D-LAW-7214-RR. We thank the principal investigators of the MODIS land surface products and AmeriFlux network. We thank the NASA Land Processes Distributed Active Archive Center (LP DAAC) for maintaining the MODIS land surface products, and the U.S. Department of Energy's Office of Science for funding the AmeriFlux data resources. MODIS land surface products were provided by the MODIS Land Science Team, at https://lpdaac.usgs.gov/dataset_discovery/modis/modis_products_table/myd15a2. Eddy covariance data were collected from the AmeriFlux network (http://ameriflux.lbl.gov/).

Appendix A. Supplementary data

Supplementary material related to this article can be found, in the online version, at doi:https://doi.org/10.1016/j.agrformet.2018.01.027.

References

Alo, C.A., Wang, G., 2010. Role of dynamic vegetation in regional climate predictions over western Africa. Clim. Dyn. 35, 907–922. http://dx.doi.org/10.1007/s00382-010-0744-z.

Anav, A., Murray-Tortarolo, G., Friedlingstein, P., Sitch, S., Piao, S., Zhu, Z., 2013. Evaluation of land surface models in reproducing satellite derived leaf area index over the high-latitude northern hemisphere. Part II: earth system models. Remote Sens. 5, 3637–3661. http://dx.doi.org/10.3390/rs5083637.

Baldocchi, D.D., Xu, L., Kiang, N., 2004. How plant functional-type, weather, seasonal drought, and soil physical properties alter water and energy fluxes of an oak-grass savanna and an annual grassland. Agric. For. Meteorol. 123, 13–39. http://dx.doi.org/10.1016/j.agrformet.2003.11.006.

Baldocchi, D.D., Wilson, K.B., 2001. Modeling CO2 and water vapor exchange of a temperate broadleaved forest across hourly to decadal time scales. Ecol. Model. 142, 155–184. http://dx.doi.org/10.1016/S0304-3800(01)00287-3.

Baldocchi, D., et al., 2001. FLUXNET: a new tool to study the temporal and spatial variability of ecosystem-scale carbon dioxide, water vapor, and energy flux densities. Bull. Am. Meteorol. Soc. 82, 2415–2434. http://dx.doi.org/10.1175/1520-0477(2001)082 < 2415:FANTTS > 2.3.CO;2.

Ball, J.T., Woodrow, I.E., Berry, J.A., 1987. A model predicting stomatal conductance and its contribution to the control of photosynthesis under different environmental conditions. Prog. Photosynth. Res. 4, 221–224. http://dx.doi.org/10.1007/978-94-017-0519-6_48.

Bonan, G.B., Levis, S., Kergoat, L., Oleson, K.W., 2002. Landscapes as patches of plant functional types: an integrating concept for climate and ecosystem models. Glob. Biogeochem. Cycles 16 (2). http://dx.doi.org/10.1029/2000GB001360.

Bunn, A.G., Goetz, S.J., 2006. Trends in satellite-observed circumpolar photosynthetic activity from 1982 to 2003: the influence of seasonality, cover type, and vegetation density. Earth Interact. 10. http://dx.doi.org/10.1175/EI190.1.

Carlson, T.N., Ripley, Da, 1997. On the relation between NDVI, fractional vegetation cover, and leaf area index. Remote Sens. Environ. 62, 241–252. http://dx.doi.org/10.1016/S0034-4257(97)00104-1.

Chen, F., Dudhia, J., 2001. Coupling an advanced land surface–hydrology model with the Penn State–NCAR MM5 modeling system. Part I: model implementation and sensitivity. Mon. Weather Rev. 129, 569–585. http://dx.doi.org/10.1175/1520-0493(2001)129 < 0569:CAALSH > 2.0.CO;2.

Ciais, P., Tans, P.P., Denning, a S., Francey, R.J., Trolier, M., Meijer, H.aJ., White, J.W.C., Berry, A., Randall, D.a, Collatz, G.J., Sellers, P.J., Monfray, P., Heimann, M., 1997. A three-dimensional ynthesis study of δ18O in atmospheric CO2: 2. Simulations with the TM2 transport model. J. Geophys. Res. Atmos. 102, 5873–5883.

Collatz, G.J., Ribas-Carbo, M., Berry, J.A., 1992. Coupled photosynthesis-stomatal conductance model for leaves of C4 plants. Aust. J. Plant Physiol. 19, 519–539. http://dx.doi.org/10.1071/PP9920519.

Collatz, G.J., Ball, J.T., Grivet, C., Berry, J.A., 1991. Physiological and environmental regulation of stomatal conductance, photosynthesis and transpiration: a model that includes a laminar boundary layer. Agric. For. Meteorol. 54, 107–136. http://dx.doi.org/10.1016/0168-1923(91)90002-8.

Diffenbaugh, N.S., 2005. Atmosphere-land cover feedbacks alter the response of surface temperature to CO2 forcing in the western United States. Clim. Dyn. 24, 237–251. http://dx.doi.org/10.1007/s00382-004-0503-0.

Ek, M.B., Mitchell, K.E., Lin, Y., Rogers, E., Grummann, P., Koren, V., Gayno, G., Tarpley, J.D., 2003. Implementation of Noah land surface model advances in the National Centers for Environmental Prediction operational Mesoscale Eta Model. J. Geophys. Res. 108, 8851. http://dx.doi.org/10.1029/2002JD003296.

Falk, M., Pyles, R.D., Ustin, S.L., Paw U, K.T., Xu, L., Whiting, M.L., Sanden, B.L., Brown, P.H., 2014. Evaluated crop evapotranspiration over a region of irrigated orchards with the improved ACASA–WRF model. J. Hydrometeorol. 15, 744–758. http://dx.doi.org/10.1175/JHM-D-12-0183.1.

Fang, H., Wei, S., Liang, S., 2012. Validation of MODIS and CYCLOPES LAI products using global field measurement data. Remote Sens. Environ. 119, 43–54. http://dx.doi.org/10.1016/j.rse.2011.12.006.

Farquhar, G.D., von Caemmerer, S., 1982. Physiological plant ecology II: water relations and carbon assimilation. In: Lange, O.L., Nobel, P.S., Osmond, C.B., Ziegler, H. (Eds.), Springer Berlin Heidelberg, Berlin, Heidelberg, pp. 549–587. http://dx.doi.org/10.1007/978-3-642-68150-9_17.

Farquhar, G.D., Lloyd, J., Taylor, J., Lawrence, B., Flanagan, J.P.S., Hubick, K.T., Wong, S.C., Ehleringer, J.R., 1993. Vegetation effects on the isotope composition of oxygen in atmospheric CO2. Nature 363, 439–443. http://dx.doi.org/10.1038/363439a0.

Fatichi, S., Pappas, C., Ivanov, V.Y., 2015. Modeling plant-water interactions: an ecohydrological overview from the cell to the global scale. Wiley Interdiscip. Rev. Water 3, 327–368. http://dx.doi.org/10.1002/wat2.1125.

Foley, Ja, Costa, M.H., Delire, C., Ramankutty, N., Snyder, P., 2003. Green surprise? How terrestrial ecosystems could affect earth's climate. Front. Ecol. Environ. 1, 38–44. http://dx.doi.org/10.2307/3867963.

Ford, T.W., Quiring, S.M., 2013. Influence of MODIS-derived dynamic vegetation on VIC-simulated soil moisture in Oklahoma. J. Hydrometeorol. 14, 1910–1921. http://dx.doi.org/10.1175/JHM-D-13-037.1.

Garrity, S.R., Bohrer, G., Maurer, K.D., Mueller, K.L., Vogel, C.S., Curtis, P.S., 2011. A comparison of multiple phenology data sources for estimating seasonal transitions in deciduous forest carbon exchange. Agric. For. Meteorol. 151, 1741–1752. http://dx.doi.org/10.1016/j.agrformet.2011.07.008.

Gifford, R.M., 1974. A comparison of potential photosynthesis, productivity and yield of plant species with differing photosynthetic metabolism. Aust. J. Plant Physiol. 1, 107. http://dx.doi.org/10.1071/PP9740107.

Goldstein, A.H., Hultman, N.E., Fracheboud, J.M., Bauer, M.R., Panek, J.A., Xu, M., Qi, Y., Guenther, A.B., Baugh, W., 2000. Effects of climate variability on the carbon dioxide, water, and sensible heat fluxes above a ponderosa pine plantation in the Sierra Nevada (CA). Agric. For. Meteorol. 101, 113–129. http://dx.doi.org/10.1016/S0168-1923(99)00168-9.

Hardwick, S.R., Toumi, R., Pfeifer, M., Turner, E.C., Nilus, R., Ewers, R.M., 2015. The relationship between leaf area index and microclimate in tropical forest and oil palm plantation: forest disturbance drives changes in microclimate. Agric. For. Meteorol. 201, 187–195. http://dx.doi.org/10.1016/j.agrformet.2014.11.010.

Hollinger, D.Y., Goltz, S.M., Davidson, E.a, Lee, J.T., Tu, K., Valentine, H.T., 1999. Seasonal patterns and environmental control of carbon dioxide and water vapour exchange in an ecotonal boreal forest. Glob. Change Biol. 5, 891–902. http://dx.doi.org/10.1046/j.1365-2486.1999.00281.x.

Jeong, S.J., Ho, C.H., Park, T.W., Kim, J., Levis, S., 2011. Impact of vegetation feedback on the temperature and its diurnal range over the Northern Hemisphere during summer in a 2 x CO2 climate. Clim. Dyn. 37, 821–833. http://dx.doi.org/10.1007/s00382-010-0827-x.

Knox, R., Bisht, G., Wang, J., Bras, R., 2011. Precipitation variability over the forest-to-nonforest transition in Southwestern Amazonia. J. Clim. 24, 2368–2377. http://dx.doi.org/10.1175/2010JCLI3815.1.

Knyazikhin, Y., Martonchik, J.V., Diner, D.J., Myneni, R.B., Verstraete, M., Pinty, B., Gobron, N., 1998a. Estimation of vegetation canopy leaf area index and fraction of absorbed photosynthetically active radiation from atmosphere-corrected MISR data. J. Geophys. Res. 103, 239–256. http://dx.doi.org/10.1029/98JD02461.

Knyazikhin, Y., Martonchik, J.V., Myneni, R.B., Diner, D.J., Running, S.W., 1998b. Synergistic algorithm for estimating vegetation canopy leaf area index and fraction of absorbed photosynthetically active radiation from MODIS and MISR data. J. Geophys. Res. 103, 32257. http://dx.doi.org/10.1029/98JD02462.

Kucharik, C.J., Barford, C.C., Maayar, M.El, Wofsy, S.C., Monson, R.K., Baldocchi, D.D., 2006. A multiyear evaluation of a dynamic global vegetation model at three AmeriFlux forest sites: vegetation structure, phenology, soil temperature, and CO2 and H2O vapor exchange. Ecol. Model. 196, 1–31. http://dx.doi.org/10.1016/j.ecolmodel.2005.11.031.

Kumar, A., Chen, F., Barlage, M., Ek, M.B., Niyogi, D., 2014. Assessing impacts of integrating MODIS vegetation data in the weather research and forecasting (WRF) model coupled to two different canopy-resistance approaches. J. Appl. Meteorol. Climatol. 53, 1362–1380. http://dx.doi.org/10.1175/JAMC-D-13-0247.1.

Lai, C.T., Katul, G., 2000. The dynamic role of root-water uptake in coupling potential to actual transpiration. Adv. Water Resour. 23, 427–439. http://dx.doi.org/10.1016/S0309-1708(99)00023-8.

Law, B.E., Arkebauer, T., Campbell, J.L., Chen, J., Sun, O., Schwartz, M., van Ingen, C., Verma, S., 2008. Terrestrial Carbon Observations: Protocols for Vegetation Sampling and Data Submission. Global Terrestrial Observing System, Rome.

Lawrence, P.J., Chase, T.N., 2007. Representing a new MODIS consistent land surface in the community land model (CLM 3.0). J. Geophys. Res. Biogeosciences 112. http://dx.doi.org/10.1029/2006JG000168.

Leuning, R., 1990. Modelling stomatal behaviour and and photosynthesis of eucalyptus grandis. Aust. J. Plant Physiol. 17, 159–175. http://dx.doi.org/10.1071/PP9900159.

Leuning, R., Zhang, Y.Q., Rajaud, A., Cleugh, H., Tu, K., 2008. A simple surface conductance model to estimate regional evaporation using MODIS leaf area index and the Penman–Monteith equation. Water Resour. Res. 44. http://dx.doi.org/10.1029/2007WR006562.

Levis, S., Foley, J.A., Pollard, D., 2000. Large-scale vegetation feedbacks on a double CO2 climate. J. Clim. 13, 1313–1325. http://dx.doi.org/10.1175/1520-0442(2000)013&1313:LSVFOA&2.0.CO;2.

Mahowald, N., Lo, F., Zheng, Y., Harrison, L., Funk, C., Lombardozzi, D., Goodale, C., 2016. Projections of leaf area index in earth system models. Earth Syst. Dyn. 7, 211–229. http://dx.doi.org/10.5194/esd-7-211-2016.

Meyers, T., Paw U, K.T., 1986. Testing of a higher-order closure model for modeling airflow within and above plant canopies. Bound.-Layer. Meteorol. 37, 297–311. http://dx.doi.org/10.1007/BF00122991.

Meyers, T.P., Paw U, K.T., 1987. Modelling the plant canopy micrometeorology with higher-order closure principles. Agric. For. Meteorol. 41, 143–163. http://dx.doi.org/10.1016/0168-1923(87)90075-X.

Moore, K.E., Fitzjarrald, D.R., Sakai, R.K., Goulden, M.L., Munger, J.W., Wofsy, S.C., 1996. Seasonal variation in radiative and turbulent exchange at a deciduous forest in Central Massachusetts. J. Appl. Meterol. http://dx.doi.org/10.1175/1520-0450(1996)035 < 0122:SVIRAT > 2.0.CO;2.

Murray-Tortarolo, G., Anav, A., Friedlingstein, P., Sitch, S., Piao, S., Zhu, Z., Poulter, B., Zaehle, S., Ahlström, A., Lomas, M., Levis, S., Viovy, N., Zeng, N., 2013. Evaluation of land surface models in reproducing satellite-derived LAI over the high-latitude northern hemisphere. Part I: uncoupled DGVMs. Remote Sens. 5, 4819–4838. http://dx.doi.org/10.3390/rs5104819.

Myneni, R.B., Hoffman, S., Knyazikhin, Y., Privette, J.L., Glassy, J., Tian, Y., Wang, Y., Song, X., Zhang, Y., Smith, G.R., Lotsch, a, Friedl, M., Morisette, J.T., Votava, P., Nemani, R.R., Running, S.W., 2002. Global products of vegetation leaf area and fraction absorbed PAR from year one of MODIS data. Remote Sens. Environ. 83, 214–231. http://dx.doi.org/10.1016/S0034-4257(02)00074-3.

Myneni, R., Knyazikhin, Y., Glassy, J., Votava, P., Shabanov, N., 2003. User' s Guide FPAR, LAI (ESDT: MOD15A2) 8-day Composite NASA MODIS Land Algorithm. FPAR, LAI User's Guid., pp. 1–17.

Niu, G.Y., Yang, Z.L., Mitchell, K.E., Chen, F., Ek, M.B., Barlage, M., Kumar, A., Manning, K., Niyogi, D., Rosero, E., Tewari, M., Xia, Y., 2011. The community Noah land surface model with multiparameterization options (Noah-MP): 1. Model description and evaluation with local-scale measurements. J. Geophys. Res. Atmos. 116, 1–19. http://dx.doi.org/10.1029/2010JD015139.

Oleson, K.W., Lawrence, D.M., Bonan, G.B., Drewniak, B., Huang, M., Charles, D., Levis, S., Li, F., Riley, W.J., Zachary, M., Swenson, S.C., Thornton, P.E., Bozbiyik, A., Fisher, R., Heald, C.L., Kluzek, E., Lamarque, F., Lawrence, P.J., Leung, L.R., Muszala, S., Ricciuto, D.M., Sacks, W., 2013. Technical Description of Version 4.5 of the Community Land Model (CLM) Coordinating. NCAR/TN-503 + STR NCAR Tech. Note.

Paw U, K.T., Gao, W., 1988. Applications of solutions to non-linear energy budget equations. Agric. For. Meteorol. 43, 121–145. http://dx.doi.org/10.1016/0168-1923(88)90087-1.

Paw U, K.T., Falk, M., Suchanek, T.H., Ustin, S.L., Chen, J., Park, Y., Winner, W.E., Thomas, S.C., Hsiao, T.C., Roger, H., King, T.S., Pyles, R.D., Schroeder, M., Matista, A.A., 2004. Carbon dioxide exchange between an old-growth forest and the atmosphere. Ecosystems 7, 513–524. http://dx.doi.org/10.1007/s10021-004-0141-8.

Privette, J.L., Myneni, R.B., Knyazikhin, Y., Mukelabai, M., Roberts, G., Tian, Y., Wang, Y., Leblanc, S.G., 2002. Early spatial and temporal validation of MODIS LAI product in the southern Africa Kalahari. Remote Sens. Environ. 83, 232–243. http://dx.doi.org/10.1016/S0034-4257(02)00075-5.

Pyles, R.D., Weare, B.C., Paw U, K.T., 2000. The UCD advanced canopy-atmosphere-soil algorithm: comparisons with observations from different climate and vegetation regimes. Q. J. R. Meteorol. Soc. 126, 2951–2980. http://dx.doi.org/10.1002/qj.49712656917.

Pyles, R.D., Weare, B.C., Paw U, K.T., Gustafson, W., 2003. Coupling between the University of California, Davis, advanced canopy–atmosphere–soil algorithm (ACASA) and MM5: preliminary results for July 1998 for Western North America. J. Appl. Meteorol. 42, 557–569. http://dx.doi.org/10.1175/1520-0450(2003)042 < 0557:CBTUOC > 2.0.CO;2.

Pyles, R., Paw U, K.T., Falk, M., 2004. Directional wind shear within an old-growth temperate rainforest: observations and model results. Agric. For. Meteorol. 125, 19–31. http://dx.doi.org/10.1016/j.agrformet.2004.03.007.

Reichstein, M., Falge, E., Baldocchi, D., Papale, D., Aubinet, M., Berbigier, P., Bernhofer, C., Buchmann, N., Gilmanov, T., Granier, A., Grunwald, T., Havrankova, K., Ilvesniemi, H., Janous, D., Knohl, A., Laurila, T., Lohila, A., Loustau, D., Matteucci, G., Meyers, T., Miglietta, F., Ourcival, J.M., Pumpanen, J., Rambal, S., Rotenberg, E., Sanz, M., Tenhunen, J., Seufert, G., Vaccari, F., Vesala, T., Yakir, D., Valentini, R., 2005. On the separation of net ecosystem exchange into assimilation and ecosystem respiration: review and improved algorithm. Glob. Change Biol. 11 (9), 1424–1439. http://dx.doi.org/10.1111/j.1365-2486.2005.001002.x.

Ryder, J., Polcher, J., Peylin, P., Ottlé, C., Chen, Y., Van Gorsel, E., Haverd, V., McGrath, M.J., Naudts, K., Otto, J., Valade, A., Luyssaert, S., 2016. A multi-layer land surface energy budget model for implicit coupling with global atmospheric simulations. Geosci. Model. Dev. 9, 223–245. http://dx.doi.org/10.5194/gmd-9-223-2016.

Sitch, S., Smith, B., Prentice, I.C., Arneth, A., Bondeau, A., Cramer, W., 2003. Evaluation of ecosystem dynamics, plant geography and terrestrial carbon cycling in the LPJ dynamic global vegetation model. Glob. Change Biol. 9, 161–185. http://dx.doi.org/10.1046/j.1365-2486.2003.00569.x.

Su, H.B., Paw U, K.T., Shaw, R.H., 1996. Development of a coupled leaf and canopy model for the simulation of plant-atmosphere interactions. J. Appl. Meteorol. 35, 733–748. http://dx.doi.org/10.1175/1520-0450(1996)035 < 0733.

Subin, Z.M., Riley, W.J., Jin, J., Christianson, D.S., Torn, M.S., Kueppers, L.M., 2011. Ecosystem feedbacks to climate change in California: development, testing, and analysis using a coupled regional atmosphere and land surface model (WRF3-CLM3.5). Earth Interact. 15, 1–38. http://dx.doi.org/10.1175/2010EI331.1.

Wharton, S., Schroeder, M., Paw U, K.T., Bible, K., Falk, M., 2009. Turbulence consideration for comparing ecosystem exchange over old-growth and clear-cut stands for limited fetch and complex canopy flow conditions. Agric. For. Meteorol. 149, 1477–1490.

Xiao, Z., Liang, S., Wang, J., et al., 2013. Use of general regression neural networks for generating the GLASS leaf area index product from time series MODIS surface reflectance. IEEE Trans. Geosci. Remote Sens. 52, 209–223.

Xiao, Z., Liang, S., Wang, T., Jiang, B., 2016. Retrieval of leaf area index (LAI) and fraction of absorbed photosynthetically active radiation (FAPAR) from VIIRS time-series data. Remote Sens. 8. http://dx.doi.org/10.3390/rs8040351.

Xu, L., Pyles, R.D., Paw U, K.T., Chen, S.H., Monier, E., 2014. Coupling the high complexity land surface model ACASA to the mesoscale model WRF. Geosci. Model Dev. Discuss. 7, 2829–2875. http://dx.doi.org/10.5194/gmdd-7-2829-2014.

Yang, W., Tan, B., Huang, D., Rautiainen, M., Shabanov, N.V., Wang, Y., Privette, J.L., Huemmrich, K.F., Fensholt, R., Sandholt, I., Weiss, M., Ahl, D.E., Gower, S.T., Nemani, R.R., Knyazikhin, Y., Myneni, R.B., 2006. MODIS leaf area index products: fromnValidation to algorithm improvement. IEEE Trans. Geosci. Remote Sens. 44, 1885–1898. http://dx.doi.org/10.1109/TGRS.2006.871215.

Yin, J., Zhan, X., Zheng, Y., Hain, C.R., Ek, M., Wen, J., Fang, L., Liu, J., 2016. Improving Noah land surface model performance using near real time surface albedo and green vegetation fraction. Agric. For. Meteorol. 218–219, 171–183. http://dx.doi.org/10.1016/j.agrformet.2015.12.001.

Zhang, X., Friedl, M.A., Schaaf, C.B., Strahler, A.H., Hodges, J.C.F., Gao, F., Reed, B.C., Huete, A., 2003. Monitoring vegetation phenology using MODIS. Remote Sens. Environ. 84, 471–475. http://dx.doi.org/10.1016/S0034-4257(02)00135-9.

Zhu, Z., Bi, J., Pan, Y., Ganguly, S., Anav, A., Xu, L., Samanta, A., Piao, S., Nemani, R.R., Myneni, R.B., 2013. Global data sets of vegetation leaf area index (LAI)3g and fraction of photosynthetically active radiation (FPAR)3g derived from global inventory modeling and mapping studies (GIMMS) normalized difference vegetation index (NDVI3G) for the period 1981 to 2. Remote Sens. 5, 927–948. http://dx.doi.org/10.3390/rs5020927.